Coronary Magnetic Resonance Angiography: Techniques and Clinical Results

13

Masaki Ishida and Hajime Sakuma

Introduction

Coronary artery disease is one of the leading causes of morbidity and mortality in many industrialized countries [1]. Catheter X-ray coronary angiography has been used as the gold standard for identifying significant luminal narrowing of the coronary arteries. However, X-ray coronary angiography entails small but definable risks [2], and a considerable number of patients undergoing elective X-ray coronary angiography are found to have no significant coronary artery disease [3]. Consequently there is a strong need for a noninvasive test that can reliably delineate narrowing of the coronary arteries.

During the past two decades, considerable progress has been made in the field of noninvasive imaging of the coronary arteries by using magnetic resonance (MR) angiography and computed tomography (CT). Contrast-enhanced multi-slice spiral CT has rapidly emerged as a noninvasive method that can provide visualization of the coronary arteries and detection of the luminal narrowing. Introduction of 64 slice CT scanners significantly improved the quality of coronary CT images in terms of both spatial and temporal resolution [4, 5]. Recent multicenter studies reported that significant coronary arterial stenosis was detected by using a 64-slice CT scanner with a sensitivity of 85–95% and a specificity of 83–90% compared with catheter X-ray coronary angiography [6, 7]. However, multi-slice CT has several disadvantages of requiring rapid injection of iodinated contrast medium and exposing patients to ionizing radiation. Due to recent technical advancements, estimated effective radiation dose of multi-slice CT coronary angiography has been dramatically reduced from 15 to 20 mSv to less than 5 mSv [4, 5, 8]. However, the radiation dose of the latest coronary CT angiography is not negligible in children and young adult patients, in addition to patients who require serial assessment of their coronary arteries. From a patient's point of view, coronary MR angiography is more preferable to coronary CT angiography for the detection of coronary artery disease, because it does not expose the patient to radiation or necessitates rapid injection of iodinated contrast material. In addition, the coronary arterial lumen can be readily visualized by coronary MR angiography in patients with heavy calcification of the atherosclerotic coronary plaques, an additional limitation of CT angiography.

Despite these potential advantages of coronary MR angiography, noninvasive MR imaging of the coronary artery is technically demanding due to the small size and tortuous course of the coronary artery and the complex motion caused by cardiac contraction and respiration. Sufficient contrast between the coronary arterial lumen and the surrounding tissue is crucial for visualization of the coronary artery. In addition, high spatial resolution and volume coverage of the coronary artery tree are required, and time available within the cardiac cycle for MR image data acquisition is limited to overcome complex motion of the coronary artery caused by cardiac contraction and respiration. In this chapter, the techniques currently used for coronary MR angiography are briefly reviewed. Then the current roles of coronary MR angiography for the evaluation of the coronary artery disease and other abnormalities such as anomalous coronary arteries and Kawasaki disease are explained. Moreover, new methods to improve visualization of the coronary artery will be updated in relation to future perspective.

Techniques of Coronary MR Angiography

Two-Dimensional and Three-Dimensional Acquisitions

Assessment of coronary artery disease with coronary MR angiography was initiated in the early 1990s by using breath-hold two-dimensional (2D)-segmented k-space gradi-

M. Ishida · H. Sakuma (✉)
Mie University Hospital, Department of Radiology, Tsu, Japan
e-mail: mishida@clin.medic.mie-u.ac.jp; sakuma@clin.medic.mie-u.ac.jp

R. Y. Kwong et al. (eds.), *Cardiovascular Magnetic Resonance Imaging*, Contemporary Cardiology,
https://doi.org/10.1007/978-1-4939-8841-9_13

ent-echo techniques [9–11]. Breath-hold 2D approach was relatively easy to implement and had some success in the visualization of the proximal coronary arteries. However, breath-hold 2D coronary MR angiography has several limitations, including slice misregistration due to inconsistent diaphragm positions between breath-held acquisitions, patient fatigue from multiple repeated breath-holdings, suboptimal signal-to-noise ratio due to 2D acquisition of thin slice, and high operator dependency to successfully image tortuous coronary arteries with 2D imaging slices. In order to overcome these limitations of breath-hold 2D methods, three-dimensional (3D) gradient-echo coronary MR angiography sequences were developed either by employing a breath-hold method or respiratory-gated method. The advantages of 3D coronary MR angiography are improved signal-to-noise ratio, volumetric coverage of the coronary arteries, and no misregistration between slices within each 3D volume acquisition. These features of 3D coronary MR angiography permit 3D post-processing of the coronary artery tree. In the past decade, volume coverage, acquisition speed, and arterial contrast of 3D coronary MR angiography were substantially improved with the use of steady-state free precession sequences and parallel imaging techniques, allowing for the acquisition of high-quality 3D MR angiograms encompassing the entire coronary arteries within a reasonably short imaging time.

The most fundamental weakness of 3D coronary MR angiography as compared with recent multi-slice CT scanners is slow acquisition speed of 3D volume data. For example, imaging of 3D data with 300 × 300 × 100 mm volume coverage and 0.6 × 0.6 × 0.6 mm acquisition resolution necessitates more than 20,000 phase encoding steps when parallel imaging factor of 2 and half scan are employed, which corresponds to approximately 1 min of non-ECG-gated imaging time with a repetition time of 3 ms. In contrast, acquisition of the same 3D volume can be completed in less than several hundred milliseconds by using area detector CT or dual-source CT. Due to slow speed constraints of MR, acquisition of 3D coronary MR angiography remains highly challenging. Several competing requirements, including optimal suppression of respiratory motion, high temporal resolution within the cardiac cycle, high spatial resolution, large 3D volume coverage, and good arterial contrast-to-noise, need to be simultaneously satisfied.

Suppression of Respiratory Motion

Breath-Hold 3D Coronary MR Angiography

In order to overcome limitations of 2D coronary MR angiography such as slice misregistration between breath-hold scans and suboptimal signal-to-noise ratio, 3D breath-hold coronary MR angiography sequences were developed [12–15]. Wielopolski et al. [11] proposed a breath-hold 3D coronary MR angiography with volume-targeted imaging (VCATS: volume coronary angiography with targeted volumes). Each coronary arterial segment was imaged with 24-mm-thick double-oblique 3D volume by using a single end-expiratory breath-hold. The entire major coronary arteries were covered in fewer than 13 breath holds. The diagnostic accuracy of the VCATS approach was evaluated in 38 patients by van Geuns et al. [15]. They found that 69% segments were assessable with this approach, and the sensitivity and specificity of 3D breath-hold MR coronary angiography for the detection of >50% luminal stenoses were 92% and 68%. Breath-hold 3D coronary MR angiography has advantages in terms of time efficiency compared with free-breathing 3D coronary MA angiography [16]. Another benefit of breath-hold 3D coronary MR angiography is that this method can utilize first-pass contrast enhancement of the coronary arterial blood following an intravenous injection of extracellular MR contrast medium such as Gd-DTPA [17–20]. Regenfus et al. obtained breath-hold 3D coronary MR angiography in 50 patients with suspected coronary artery disease, by injecting extracellular MR contrast medium at a flow rate of 1 ml/s immediately prior to breath-hold 3D acquisitions [20]. The sensitivity and specificity were 94% and 57% for detecting patients having significant coronary artery disease with contrast-enhanced breath-hold 3D coronary MR angiography.

Breath-hold 3D coronary MR angiography has several limitations. Short imaging time of breath-hold 3D acquisition is achieved at the expense of spatial resolution and 3D volume coverage. In addition, many patients with heart disease or pulmonary disease cannot hold their breath for a long time. Another important limitation of breath-hold MR acquisition is that breath-holding does not eliminate motion of the diaphragm. A continued drift of the diaphragm position was observed during breath-holding which can cause significant blurring on breath-hold 3D coronary MR angiography [21].

Free-Breathing 3D Coronary MR Angiography

Free-breathing, respiratory-gated 3D coronary MR angiography is currently the most commonly used MR approach for the assessment of coronary arteries in patients with heart disease. Respiratory bellows belt were initially used to obtain free-breathing coronary MR angiography [21, 22]. Oshinski et al. reported that free-breathing 2D coronary MR angiography with respiratory belt provides improved resolution, aligned sections of coronary arteries, and improves patient tolerance [22]. However, respiratory motion artifacts and blurring were inevitable with respiratory bellows belt because it cannot detect drift of the diaphragm position. Free-breathing coronary MR angiography has been substantially improved with respiratory navigators which measure the position of the right lung-diaphragm interface by using

MR signal. The initial implementations of free-breathing 3D coronary MR angiography were based on retrospective navigator gating [23–26]. With retrospective navigator echo sequences, image data were over sampled by acquiring each phase encoding step data several times regardless of the respiratory motion. During reconstruction, only image data acquired within a respiratory gating window were used for generating coronary MR angiography. Retrospective navigator gating has been replaced by a prospective real-time navigator gating method [27–30]. Current free-breathing 3D coronary MR angiography sequences utilize radiofrequency excitation pulse to excite a column of tissue perpendicular to the right lung-diaphragm interface (Fig. 13.1). In each cardiac cycle, both navigator echo data for respiratory gating and image data were acquired. If position of the lung-diaphragm interface is within a predefined acceptance window (typically ±2.5 mm) at the end-expiratory level, image data are accepted and stored for image reconstruction. Otherwise, image data are rejected and acquisition is repeated in the next cardiac cycle. Coronary MRA data acquisition is continued until all necessary data in k-space are collected. In addition to respiratory gating, navigator echo data is used for adaptive real-time motion correction of 3D imaging volume [27–31]. If the lung-diaphragm interface is within an acceptance window, the superior-to-inferior position of 3D acquisition volume is corrected on a real-time basis by utilizing the positional offset information of the lung-diaphragm interface measured by navigator echo.

There are several advantages in free-breathing 3D coronary MR angiography with prospective navigator gating. Since there is no constraint of imaging time caused by breath-holding, 3D coronary MR images can be acquired with improved spatial resolution, larger 3D volume overage of the coronary artery tree, and improved signal-to-noise. The major disadvantage of free-breathing 3D coronary MR angiography is a long scan time, which typically ranged from several minutes to 15 min. Another limitation is that acquisition of free-breathing 3D coronary MR angiography often fails in patients with irregular breathing pattern and those showing a drift of diaphragm position over time. To overcome this problem, several approaches have been proposed. First, the use of 32-channel cardiac coils and a higher parallel imaging factor has been proposed. In a study by Nagata et al., the mean imaging time of whole-heart coronary MRA at 1.5 T significantly reduced from 12.3 ± 4.2 min with five-channel coils to 6.3 ± 2.2 min by using 32-channel coils [32]. The reduction of imaging time leads to an improved study success rate (100%) without noticeable worsening of image quality [32]. Second, the abdominal belt helps to shorten the imaging time of whole-heart coronary MRA because it reduces the amplitude of diaphragmatic position and improves scan efficiency (Fig. 13.2). A recent

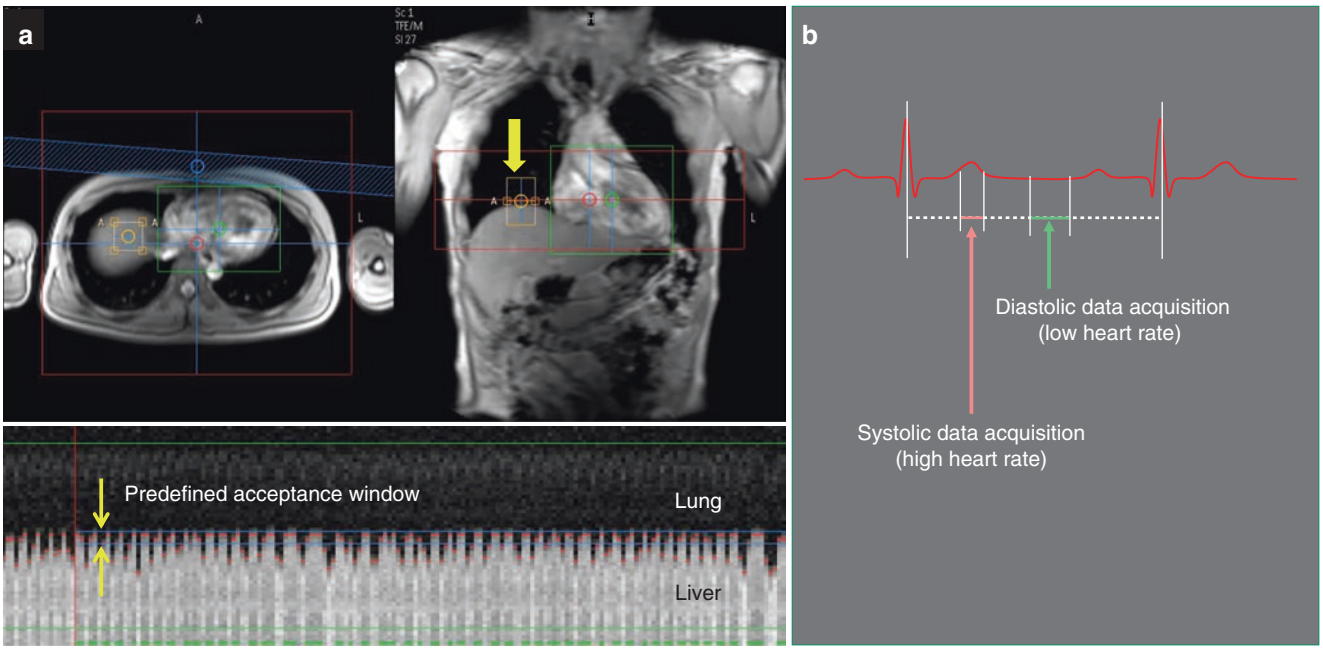

Fig. 13.1 Respiratory-gated acquisition with a prospective real-time navigator echo method. (**a**), A selective 2D radiofrequency excitation pulse to excite a column of tissue perpendicular to the right lung-diaphragm interface. If position of the lung-diaphragm interface is within a previously defined acceptance window at the end-expiratory level, image data are accepted and stored for image reconstruction. (**b**), Coronary MR angiography can be acquired either in end-systole or during diastole. In patients with a high heart rate, narrow acquisition window is critically important for reducing motion blurring of the coronary MRA. Even in patients with low heart rate, narrow acquisition window of 30–50 ms is helpful to obtain sharp coronary MR angiograms

Fig. 13.2 The 20-cm wide abdominal belt was wrapped tightly around the patient's abdomen during end-expiration to suppress diaphragmatic motion

study by Ishida et al. showed that the application of the abdominal belt significantly improved scan efficiency and image quality of navigator-gated whole-heart coronary MRA both in the UK and Japanese patient population [33].

Suppression of Cardiac Motion

X-ray coronary angiography can provide high-resolution images of the coronary artery real time without using cardiac gating or respiratory gating, because acquisition time per image frame is short enough (<20 ms) to eliminate motion blurring of the coronary artery. In contrast, electrocardiographic (ECG) gating is required in coronary MR angiography because MR imaging time is too long to freeze the motion of the coronary artery by cardiac contraction and diastolic relaxation. In most initial studies of coronary MR angiography, image data were acquired during mid-diastolic phase by using a fixed delayed time after ECG R-wave trigger. However, the optimal delay time and width of acquisition window in the cardiac cycle to minimize coronary arterial motion is different from patient to patient. Therefore, both trigger delay time and acquisition window in the cardiac cycle should be optimized in each patient. Stuber et al. proposed the following equation to calculate the delay after R-wave trigger to start data acquisition: $Td = [(tRR - 350) \times 0.3] + 350$, where tRR refers to the time between two consecutive ECG R-waves [34]. This equation is based on a principle in cardiac physiology that the systolic duration in the cardiac cycle remains relatively constant and the diastolic duration is reduced as the heart rate increases. The approach using this equation allows for an automated calculation of the acquisition delayed time in the cardiac cycle. However, the rest period of the coronary artery in the cardiac cycle is substantially different in each patient depending not only on patients' heart rate but also other hemodynamic factors, which may cause inconsistent image quality of coronary MR angiography with the standardized ECG trigger delay calculated form heart rate [35]. The use of subject-specific data acquisition window in the cardiac cycle is recommended to improve quality of coronary MR angiography and is especially critical for the visualization of the right coronary artery [36], since the right coronary artery moves more than twice as much as the left coronary arteries. There are several approaches to determine a subject-specific acquisition window in the cardiac cycle. Wang et al. proposed an ECG-triggered M-mode navigator echo technique to monitor cardiac motion and identify the period of minimal cardiac motion in the cardiac cycle [35]. Recently, high temporal resolution cine MR images acquisition is more commonly performed in order to determine the subject-specific data acquisition window in the cardiac cycle [37]. A trigger delay time and an interval of minimal motion of the coronary artery are visually determined on cine MR images for the subsequent coronary MR angiography acquisition, typically by referring the RCA.

Free-breathing acquisition with the navigator echo technique allows for the use of narrow acquisition windows in the cardiac cycle that can effectively reduce motion blurring of the coronary artery. However, as the acquisition window is shortened, the overall scan time is prolonged. Higher parallel imaging factor achieved by 32-channel cardiac coils can reduce overall data acquisition time of coronary MRA, which can be utilized not only to reduce total study time but also to narrow the acquisition window in the cardiac cycle without extending the scan time. In a study reported by Nagata et al., the mean acquisition window in the cardiac cycle by using 32-channel cardiac coils and parallel imaging factor of 4 (84 ± 57 ms for diastolic acquisition and 48 ± 18 ms for systolic acquisition) was approximately half of that in a previous study using 5-channel cardiac coils (152 ± 67 ms for diastolic acquisition and 98 ± 26 ms for systolic acquisition), while the success rate, image quality, and overall scan time were substantially improved [32, 38]. In patients with a high heart rate, narrow acquisition window in the cardiac cycle (<50 ms) is critically important for reducing motion blurring of the coronary artery on whole-heart coronary MRA. It should be noted that even in patients with low heart rate, narrow acquisition window of 30–50 ms is helpful to obtain sharp coronary MR angiograms.

Contrast of the Coronary Artery

Pulse Sequence and Magnetic Field Strength

On 2D gradient-echo coronary MR angiography, high luminal blood signal is primarily generated by the in-flow effect of unsaturated blood spins flowing into thin 2D imaging slice. Although an introduction of 3D gradient-echo coronary MR

angiography eliminates many of the drawbacks of 2D coronary MR angiography, 3D gradient-echo approach has one significant downside, that is, reduced in-flow effect. Blood spins in thick 3D volume is progressively saturated by repeated radiofrequency excitations, and the arterial blood signal intensity on 3D gradient-echo coronary MR angiography is substantially attenuated when 3D imaging volume is large. Therefore, relatively thin 3D volume (2–3 cm total thickness) targeting one of the major coronary arteries is preferable to 3D gradient-echo coronary MR angiography [29, 30].

3D coronary MR angiography sequences with steady-state free precession acquisition (true FISP, fast imaging in steady-state precession; balanced TFE, balanced turbo field echo; FIESTA, fast imaging employing steady-state acquisition) permit acquisition of MRA images with high blood contrast without administration of MR contrast media. Because steady-state free precession sequence is sensitive to magnetic field inhomogeneities, short repetition time, and volume shimming capability to achieve homogeneous magnetic field in the imaging volume are important to obtain good coronary MR angiograms. With steady-state free precession sequences, the blood signal intensity on 3D coronary MR angiography is considerably higher than that of 3D gradient-echo sequence [39, 40]. As a result, 3D coronary MR angiography with steady-state free precession acquisition is not dependent on in-flow effect and excellent 3D coronary MR angiograms with high blood signal can be obtained by using thick 3D volume coverage. Image quality of 3D steady-state coronary MR angiography is further improved with an optimization of k-space sampling strategy. Reduced motion artifacts and superior vessel sharpness were observed with the 3D steady-state coronary MR angiographic sequence with radial k-space sampling when compared with those by cartesian 3D steady-state coronary MR angiography and 3D gradient-echo coronary MR angiography [41].

Whole-heart coronary MR angiography using a free-breathing 3D steady-state free precession has been introduced as a method that can provide visualization of all three major coronary arteries with a single 3D acquisition [42] (Figs. 13.3 and 13.4). Steady-state free precession sequences permit acquisition of thick 3D axial volume that encompasses the entire heart without losing arterial contrast. By using this whole-heart approach, one can visualize all three major coronary arteries with a reduced total examination time in comparison with targeted double-oblique 3D gradient-echo MR angiography. In addition, planning of whole-heart coronary MR angiography is quite simple, which eliminates time-consuming 3-point planning that was required for the targeted double-oblique approach. Although 3D coronary MR angiography using targeted double-oblique acquisitions demonstrated relatively good accuracy for identifying stenoses in the proximal and middle coronary arterial segments, coverage of the distal segments was often limited. For example, the proportion of assessable segments was 68% for the middle left circumflex artery with targeted double-oblique 3D coronary MR angiography [30]. With the whole-heart approach, long segments of all major coronary arteries can be imaged. The proportion of distal segments exhibiting good or excellent image quality was over 90% for all major coronary arteries in our study using the whole-heart approach [32, 38, 43].

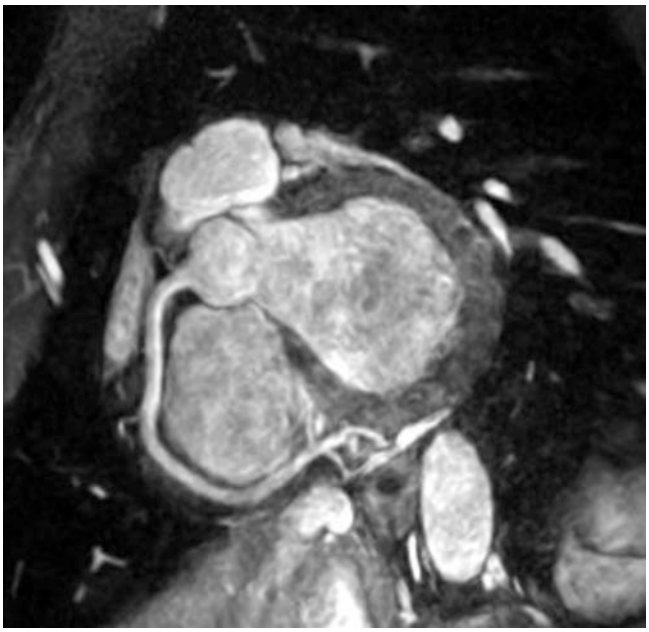

Fig. 13.3 Free-breathing 3D coronary MR angiography of the right coronary artery acquired with a steady-state free precession sequence (balanced TFE) with fat saturation and T2 preparation and a double-oblique targeted volume approach. Respiratory gating was performed with a prospective real-time navigator echo technique. Three-point planning was used to define double-oblique 3D slices parallel to the right coronary artery. No stenosis in the coronary artery is demonstrated in this case

Steady-state free precession (SSFP) sequences are generally preferred to gradient-echo sequences at 1.5 T because the high T2/T1 ratio of the blood acts as an intrinsic contrast medium for SSFP coronary and helps to increase the blood signal on non-contrast-enhanced coronary MRA [39, 40] (Figs. 13.5 and 13.6). Higher magnetic field strength at 3 T is increasingly used for cardiac MRI, because high-field MR imaging can provide improved SNR [44, 45]. The difficulties of 3 T cardiac MRI include increased off-resonance effect caused by magnetic field inhomogeneity and high specific adsorption rate (SAR). As the result, coronary MRA using SSFP acquisition is particularly challenging at higher field strength, because SSFP sequence is susceptible to inhomogeneity of magnetic field and requires higher flip angles to obtain enough contrast between the blood and the myocardium. Consequently, at 3 T, gradient-echo sequences are generally preferred to SSFP for coronary MRA acquisition [46] (Fig. 13.7).

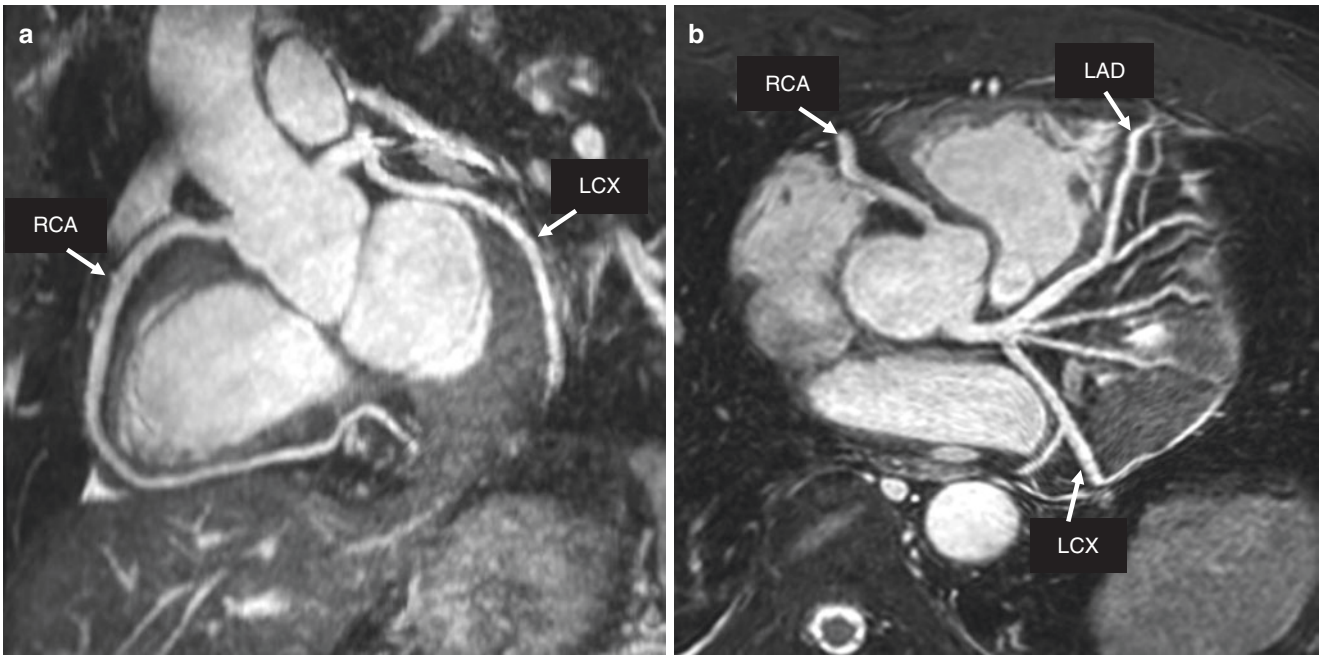

Fig. 13.4 Free-breathing, navigator echo-gated whole-heart coronary MR angiography acquired with a steady-state free precession sequence (balanced TFE) with fat saturation and T2 preparation in a subject with normal coronary artery. (**a**), Left anterior oblique whole-heart coronary MR angiogram reformatted with curved multi-planar reformatting clearly depicts the right coronary artery (RCA) and left circumflex (LCX) arteries. (**b**), Oblique axial whole-heart coronary MR angiogram reformatted with curved multi-planar reformatting visualizes the left main coronary artery, left anterior descending (LAD) artery, proximal RCA and LCX arteries [43]. (Reprinted with permission from Sakuma et al. [43], Copyright 2005, with permission from Radiological Society of North America)

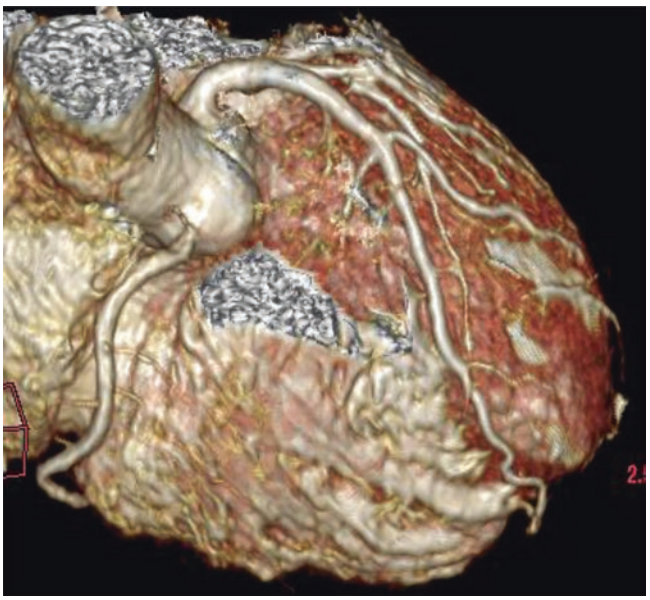

Fig. 13.5 Whole-heart coronary MR angiography acquired with a free-breathing steady-state free precession sequence in a subject with normal coronary artery. Volume rendering image of whole-heart coronary MR angiography is useful for three-dimensional anatomical recognition of the right coronary artery, left anterior descending artery, and its branches

Recently an interesting findings were reported by Soleomanifard et al., demonstrating that the 3D bSSFP acquisition, using advances in 3.0 T MR scanner equipped with recently available technologies such as multi-transmit, 32-channe cardiac coil, and localized B0 and B1+ shimming, provides high-quality noninvasive imaging of the proximal to distal segments of the major coronary arteries employing a single breath-hold volume-targeted coronary MRA [47].

Preparation Pulses for Ensuring Sufficient Image Contrast

The contrast between luminal blood and surrounding tissue needs to be maximized for the better delineation of the coronary artery on MR angiography. With "bright blood" coronary MR angiography, the pulse sequences are designed to enhance the signal from coronary arterial blood and to suppress the signal from the surrounding structures such as pericardial fat and myocardium [10]. In contrast to 3D time-of-flight MRA of the cerebral arteries, in-flow effect of the arterial blood is less prominent on coronary MRA. Therefore, suppression of the signal from the surrounding structures such as pericardial fat and myocardium is important to obtain sufficient arterial contrast on coronary MRA [10, 48]. Suppression of fat signal can be achieved by

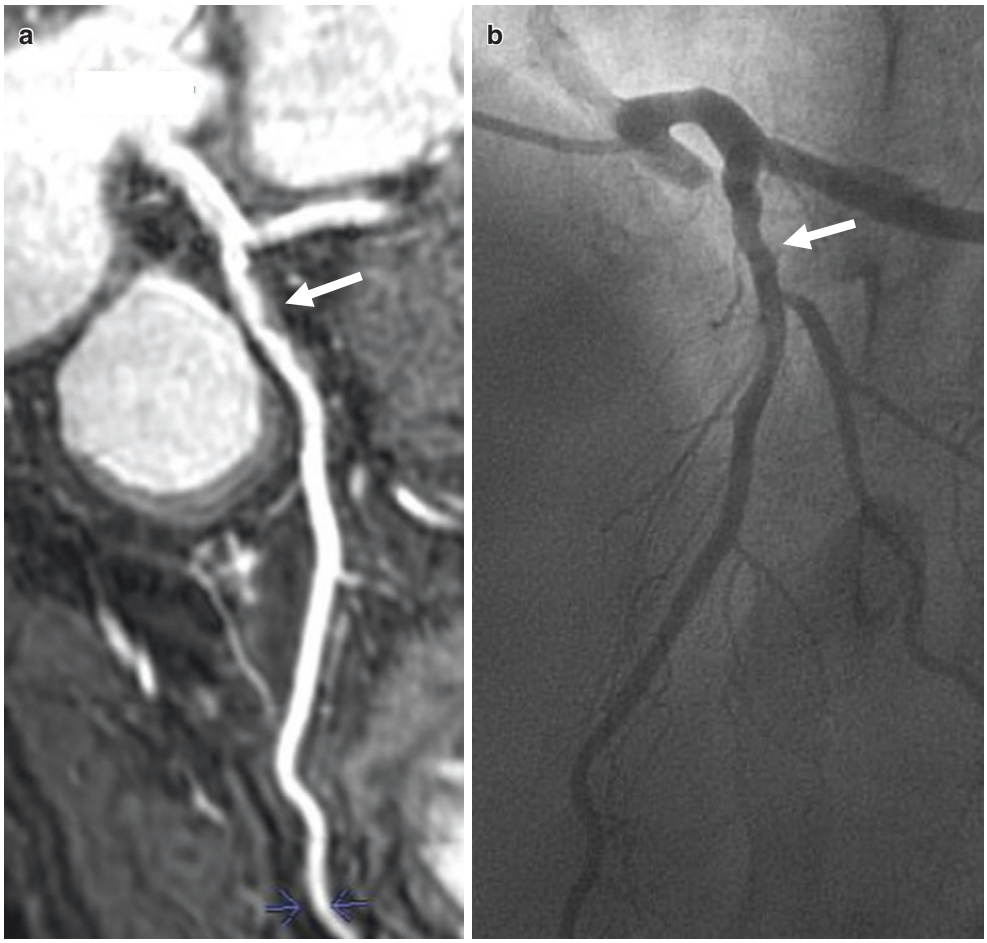

Fig. 13.6 Whole-heart coronary MR angiography acquired with a free-breathing, steady-state free precession sequence in a patient with suspected coronary artery disease. (**a**) Curved multi-planar reformatted image of whole-heart coronary MR angiography clearly reveals proximal and distal segments of the left anterior descending artery. Although no significant luminal narrowing is observed, MR image reveals the presence of atherosclerotic plaque in the coronary arterial wall (arrow). (**b**) X-ray coronary angiography in the same subject

applying a fat saturation pulse that selectively saturates the longitudinal magnetization of fat spins prior to image acquisition. Another alternative approach to suppress fat signal is use of a spectral selective radiofrequency pulse that selectively excites water spins. Currently fat saturation pulses are more widely used because short repetition time, which is critical to obtain good coronary MR angiographic images with steady-state free precession sequences, is more easily achieved. Recently, highly resolved, dual-echo Dixon CMRA approaches have been developed to enhance CMRA image quality by improved fat suppression and to provide additionally fat-only information [49]. In their study, it has been shown that Dual-echo Dixon can help to improve whole-heart CMRA image quality significantly. The additional whole-heart fat information delivered by this approach also has a potential to evaluate the diagnostic and the predictive value of intramyocardial and extramyocardial fatty deposits.

Suppression of myocardial signal is important for the visualization of distal coronary arteries and branch arteries. A T2-weighted magnetization preparation pulse is used to suppress myocardial signal [28]. Another advantage of T2 preparation pulse is a suppression of venous blood signal in the epicardial veins. T2 relaxation time of deoxygenated venous blood is substantially shorter than that of oxygenated arterial blood, resulting in the reduction of venous blood signal with T2 preparation pulse.

This T2 preparation prepulse is commonly applied without spatial selection to minimize flow sensitivity, but the nonselective implementation results in a reduced magnetization of the in-flowing blood and a related penalty in signal-to-noise ratio. Soleimanifard et al. have proposed the use of spatially selective T2 preparation prepulse where the user could freely adjust angulation and position of the T2Prep slab to avoid covering the ventricular blood pool and saturating the in-flowing spins [47]. They demonstrated that the spatially selective T2Prep increased in vivo human coronary artery signal-to-noise ratio (42.3 6 2.9 vs. 31.4 6 2.2, n 5 22, $P < 0.0001$) and contrast-to-noise ratio (18.6 6 1.5 vs. 13.9 6 1.2, P 5 0.009) as compared to those of the nonselective T2Prep [47].

Contrast Medium

Administration of T1 shortening MR contrast medium is useful to improve blood contrast on 3D gradient-echo coronary MR angiography. In the presence of T1 shortening MR

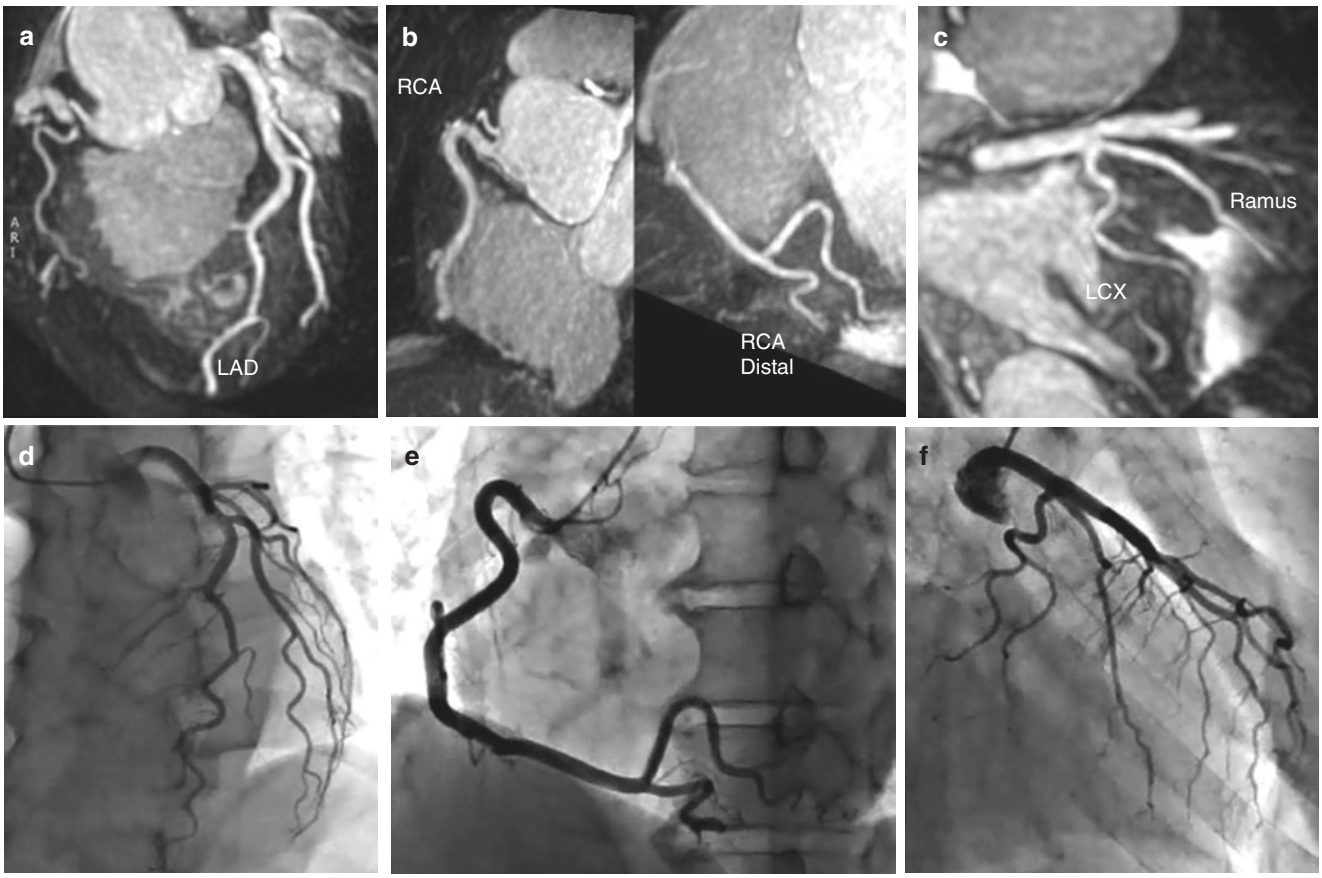

Fig. 13.7 Thin-slab maximum-intensity projection images of whole-heart coronary MR angiography acquired with a gradient-echo sequence in a subject with normal coronary artery at 3.0 tesla MR imager for the left anterior descending artery (LAD) (**a**), right coronary artery (RCA) (**b**), and circumflex artery (LCx) (**c**). MRA data was acquired after late gadolinium contrast-enhance MRI (0.15 mmol/kg) using T1-weighted gradient-echo sequence with T2 preparation and SPIR. Corresponding X-ray coronary angiogram was demonstrated (**d–f**)

contrast medium, magnetization of blood spins rapidly recovers after radiofrequency pulse, preventing saturation of the blood signal. With sufficient blood concentration of MR contrast medium, the blood signal intensity is primarily determined by T1 relaxation time of the blood instead of inflow effect, and one can utilize high radiofrequency flip angle to maximize the blood signal. In addition, contrast enhancement allows for acquiring 3D gradient-echo coronary MR angiograms with large 3D volume coverage. There are three different types of contrast medium currently available, as follows: (1) extracellular contrast medium [20], (2) intravascular contrast medium [50], and (3) slightly albumin-binding contrast medium [51]. Conventional extracellular contrast medium exhibits nonspecific distribution in the extracellular space and rapidly extravasates from intravascular space to the interstitial space after intravenous administration. Sufficient T1 shortening of the blood is only maintained during the first pass following venous administration [17, 18]. In contrast, intravascular MR contrast media remain in the blood pool longer than the extravascular contrast media. These intravascular contrast media, either iron particles [52, 53] or gadolinium molecules with [54, 55] and without albumin-binding [56], are distributed in the blood pool and exhibited greater T1 shortening effects in comparison with conventional extracellular contrast media. Slightly albumin-binding contrast medium exhibits relatively prolonged retention time in the blood and high relaxivities [57] while maintaining late enhancement abilities [58]. Several investigators have demonstrated that administration of intravascular or slightly albumin-binding agent is highly useful in improving arterial contrast on 3D gradient-echo coronary MR angiography [51–56]. When sufficient shortening of T1 relaxation time of the blood is achieved by administration of intravascular agent or high-dose slightly albumin-binding agent, gradient-echo MRA with inversion-recovery prepulse exhibits high blood contrast as well as good fat saturation. Recently, Raman et al. performed an intraindividual comparison of intravascular contrast agent, gadofosveset (0.03 mmol/kg), and extracellular agent, Gd-BOPTA (0.1 mmol/kg), for free-breathing 3D coronary MRA at 3.0 T using a relatively slow injection scheme with 20 mL saline flush at a flow rate of 0.66 mL/s [59]. They conclude that the

use of an intravascular contrast agent performed as well as, or slightly better than, a primarily extravascular extracellular contrast agent for coronary MRA at 3 T [59].

Recent Improvements in Acquisition Speed and Resolution

Imaging Acceleration with Parallel Imaging Techniques

Imaging speed is very important not only for breath-hold 3D coronary MR angiography but also for free-breathing 3D coronary MR angiography, as reduced scan time leads to improved study success rate and higher patient throughput. Parallel imaging techniques in image space such as SENSE (sensitivity encoding) or in k-space such as generalized autocalibrating partially parallel acquisition (GRAPPA) and simultaneous acquisition of spatial harmonics (SMASH) enable substantial scan time reduction in cardiac MR imaging [60–62] and are now widely used to reduce scan time of clinical 3D coronary MR angiography. The major drawback of using fast imaging techniques such as parallel imaging and half scan is loss of signal-to-noise ratio. Therefore, it is important to have an appropriate balance between speed and image quality when determining imaging parameters of coronary MR angiography. Multichannel coils and high-field MR system are two approaches that can provide substantial improvement in the signal-to-noise ratio of coronary MR angiography. In a study by Reeder et al., 32-channel cardiac coils demonstrated significantly improved signal-to-noise ratio and geometry factor, which permits to use parallel imaging acceleration factor of up to 4 [63], while the acceleration rates using 5–16 element cardiac-coil arrays is up to twofold.

High-Field Coronary MR Angiography for Improved Resolution and SNR

There has been an increasing interest in high-field coronary MR angiography, because signal-to-noise ratio increases approximately linearly with field strength, and substantial improvement in signal-to-noise ratio is expected with a magnetic field strength of 3.0 T [45, 46]. This gain in signal-to-noise ratio enables the acquisition of images with higher spatial resolution or reduced imaging time, both of which are especially important in coronary MR angiography. In 2002, Stuber et al. demonstrated the feasibility of human coronary MR angiography using a 3.0 T MR imager [44]. There are several important impediments to high-field cardiac imaging, which include high radiofrequency power deposition quadratically increased with field strength, susceptibility-related local magnetic field variations, increased sensitivity to motion artifacts, impaired ECG R-wave triggering due to augmented magnetohydrodynamic effects. However, 3.0 T MR imager has become a platform of choice for high-resolution coronary MR angiography because whole-heart coronary MR angiography at 3.0 T has shown significantly improved image quality and diagnostic accuracy as compared with those at 1.5 T with a use of gadolinium contrast administration and gradient-echo sequence [36, 59]. Recently, excellent volume-targeted coronary MR angiograms with submillimeter spatial resolution ($0.35 \times 0.35 \times 1.5$ mm^3) were demonstrated at 3.0 T, allowing for improved detection of stenosis [64]. However, such high-resolution targeted acquisitions require a 9-min scan time per vessel assuming 100% navigator gating efficiency. Thus, further imaging acceleration technique will be desirable.

Clinical Applications of Coronary MR Angiography

Anomalous Coronary Arteries

Anomalous origin of the coronary artery is relatively uncommon but important cause of chest pain and sudden cardiac death. The incidence of anomalous coronary arteries in subjects without known congenital heart disease was reported to be 0.3–0.9% [65, 66]. Among various types of anomalous coronary arteries, the coronary arteries that pass between the aorta and pulmonary artery have a potential to impair myocardial perfusion and can cause sudden death. The diagnostic method of choice for detecting coronary artery anomalies has been catheter X-ray coronary angiography. However, X-ray coronary angiography provides only a 2D view of a vessel's complex 3D path and is associated with several limitations including invasiveness and radiation exposure. Coronary MR angiography has been shown to have high sensitivity and specificity for detecting anomalous coronary arteries and for delineating proximal courses of the vessels [67–69] (Fig. 13.8). A recent study demonstrated that anomalous coronary arteries can be accurately assessed by contrast-enhanced multi-slice CT as well [70]. However, coronary MR angiography seems to be more preferable to CT, because many patients with suspected anomalous coronary arteries are in younger age and MR angiography can provide equivalent diagnostic information for the detection of anomalous coronary arteries and for the identification of their proximal courses without exposing the patients to radiation.

Kawasaki Disease

Kawasaki disease is an acute febrile illness with mucosal inflammation, skin rash, and cervical lymphadenopathy in young children [71] and produces coronary artery aneurysms in up to 25% of untreated cases. Size of coronary artery aneurysm often changes over time and is correlated with the risk of

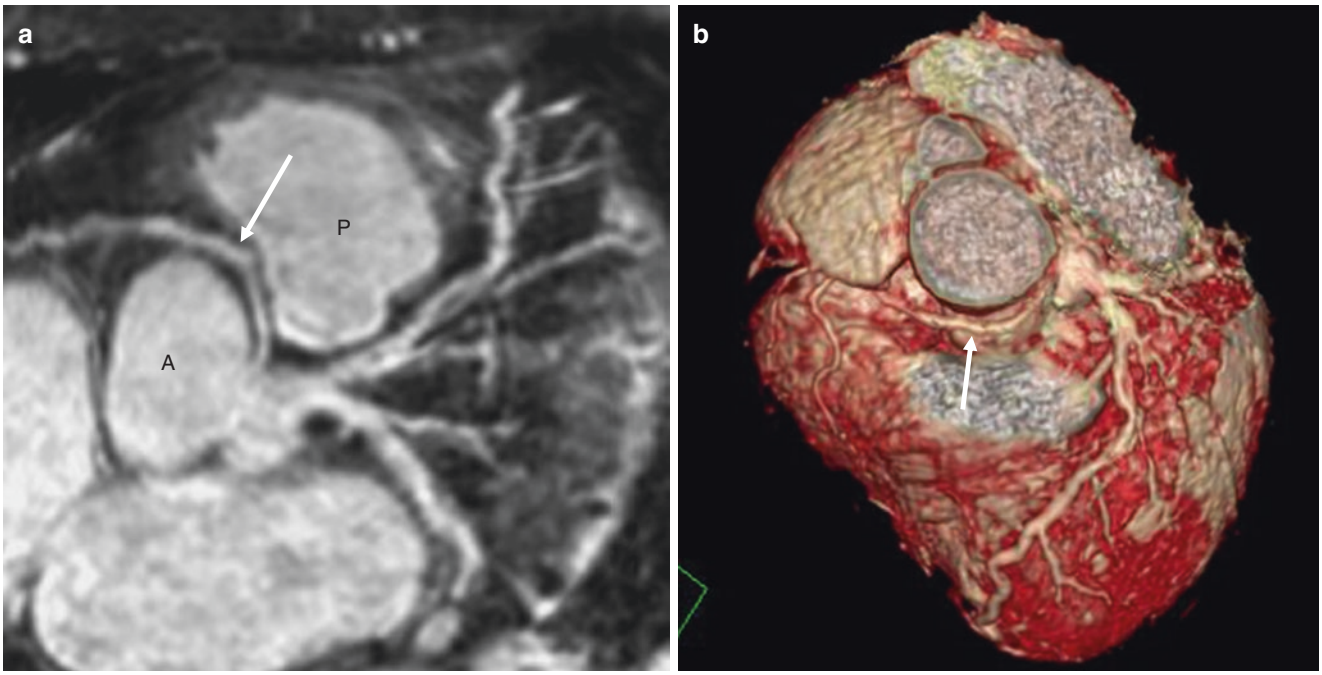

Fig. 13.8 Whole-heart coronary MR angiography in a patient with anomalous right coronary artery. Curved multi-planar reformatted MR angiographic image (**a**) and volume rendering image (**b**) demonstrate that the anomalous right coronary artery arises from the left sinus of Valsalva. The proximal course of the right coronary artery with anomalous origin (arrow) is located between the aortic root (A) and right ventricular outflow tract to proximal pulmonary artery (P)

coronary thrombosis and development of coronary artery stenoses. Thus, serial assessment of aneurismal size is important in risk stratification and therapeutic management. Serial evaluation with X-ray angiography in children carries risks associated with invasive catheterization and exposure to ionizing radiation. Transthoracic echocardiography is widely used and is often sufficient for the assessment of coronary artery aneurysm in young children. As children grow, however, visualization and characterization of the coronary artery become more difficult. Coronary MR angiography provides noninvasive detection and size measurement of coronary artery aneurysms in patients with Kawasaki disease and can be used as an alternative imaging method when image quality of transthoracic echocardiography is insufficient [72] (Fig. 13.9). Another recent study demonstrated that MR coronary angiography and X-ray coronary angiography shows excellent agreement in the diagnosis of coronary artery aneurysm, and the maximal diameter and length of the aneurysm by MR angiography and X-ray coronary angiography were similar [73].

Coronary Artery Disease

Diagnostic Accuracy of Visual Assessment of Coronary MRA

Detection of coronary arterial stenoses with coronary MR angiography is challenging, because sufficient spatial resolution is required to correctly identify luminal narrowing of the coronary artery. Table 13.1 summarizes the sensitivity and specificity of coronary MR angiography for the detection of coronary arterial stenoses in representative previous studies [10, 15, 20, 26, 30, 32, 74–80]. The sensitivity (50–96%) and specificity (42–97%) of coronary MR angiography for predicting coronary artery stenoses on X-ray coronary angiography were considerably variable in these studies. Because coronary MR angiography sequences have undergone considerable technical improvements over the past 20 years, the diagnostic accuracy of coronary MR angiography has significantly improved over time.

The first multicenter study was reported by Kim and colleagues by using free-breathing, navigator-gated 3D gradient-echo coronary MR angiography [30]. In this study, 109 patients with suspected coronary artery disease were evaluated, and 84% (636/759) of the proximal and middle coronary artery segments were interpretable on MR angiography. The sensitivity and specificity of coronary MR angiography for identifying a patient as having significant coronary artery disease were 93% and 42%. In the subgroup of patients with the left main coronary artery disease or three-vessel disease, coronary MR angiography demonstrated the sensitivity of 100% and the specificity of 85%, indicating the value of free-breathing 3D coronary MRA for excluding severe coronary artery disease.

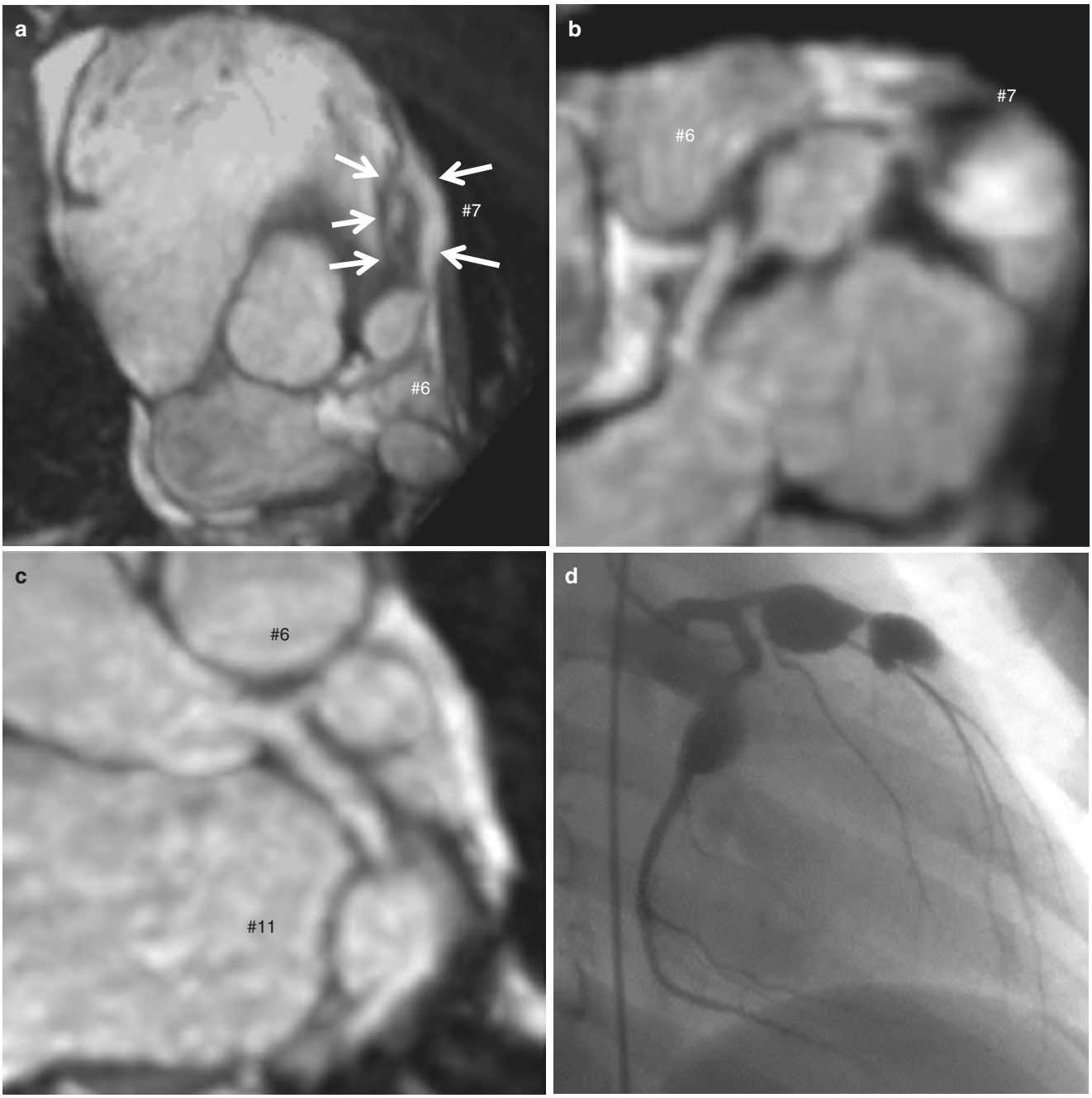

Fig. 13.9 Whole-heart coronary MR angiogram in an 8-year-old boy with Kawasaki disease. (**a**–**c**), Thin-slab maximum-intensity projection images of coronary MRA demonstrates multiple aneurysms in LAD and LCx. It should be noted that partial luminal thrombus is visualized demonstrated in the aneurysm located on LAD #7, which is confirmed on invasive X-ray angiography (**d**)

An introduction of steady-state free precession sequences has considerably improved contrast of 3D coronary MR angiography, because steady-state sequences can provide inherently high blood signal intensity without using MR contrast medium. Jahnke et al. compared the diagnostic performances of breath-hold 3D coronary MR angiography and free-breathing coronary MR angiography by using the steady-state free precession sequence, double-oblique targeted volume acquisition [81]. They found that more coronary artery segments were assessable with free-breathing coronary MR angiography (79%) than breath-hold coronary MR angiography (45%). In addition, free-breathing coronary MRA angiography was superior to breath-hold coronary MR angiography both in terms of image quality and diagnostic accuracy, with overall sensitivity and specificity of 72% and 92% by free-breathing approach and 63% and 82% by breath-hold approach.

Table 13.1 Detection of significant coronary arterial stenoses with coronary MR angiography in representative previous studies [10, 15, 20, 26, 30, 32, 74–80]

Investigator	Reference	Method	Sensitivity (%)	Specificity (%)
Manning WJ	NEJM 1993;328:828 [10]	2D breath-hold	90	92
Duerinckx AJ	Radiology 1994;193:731 [74]	↑	63	82
Van Geuns RJ	Radiology 2000;217:270 [15]	3D breath-hold	68	97
Regenfus M	JACC 2000;36:44 [20]	↑	94	57
Woodard PK	AJR 1998;170:883 [26]	3D navigator, retrospective	73	N/A
Sandstede JJ	AJR 1999;172:135 [75]	↑	81	89
Sardanelli F	Radiology 2000;214:808 [76]	↑	82	89
Kim WY	NEJM 2001;345:1863 [30]	3D navigator, prospective	93	42
Bogaert J	Radiology 2003;226:770 [77]	↑	50	90
Kefer J	JACC 2005;46:92 [78]	↑	75	77
Kato S	JACC 2010;56:983 [79]	↑	88	72
Nagata M	Radiology 2011;259:384 [32]	↑	87	86
Yang Q	Circ Cardiovasc Imaging 2012;5:573 [80]	↑	96	87

Free-breathing coronary MR angiography with axial 3D slices covering the whole-heart has become feasible by utilizing a navigator-gated 3D steady-state free precession sequence. Whole-heart coronary MR angiography can provide visualization of the entire coronary artery trees in a single 3D acquisition [38, 42, 43, 82]. An initial study in our group demonstrated that acquisition of whole-heart coronary MR angiography was successful in 34 (87.2%) of 39 patients, with the averaged acquisition duration of 13.8 ± 3.8 min [43]. In addition, long segments of all major coronary arteries including the distal segments can be imaged. The sensitivity and specificity of 1.5 T whole-heart coronary MR angiography in 20 patients for detecting patients having at least one coronary arterial stenosis were 83.3% and 75.0% in this initial study.

For the further improvement of detection of coronary artery disease, whole-heart coronary MR angiography was acquired in 131 patients by using an optimized acquisition window [38]. In contrast to our previous study, a patient-specific acquisition window was set either during systole or during diastole, depending on the phase of minimal motion of the right coronary artery on cine MR images. Coronary MR angiograms were acquired during diastole in 83 patients (delay after R-wave trigger, 627 ms ± 64) and during systole in 48 patients (delay after R-wave trigger, 259 ms ± 39). The study success rate of whole-heart coronary MR angiography (86%) was not improved by using an optimized patient-specific acquisition window either during systole or diastole. However, the sensitivity, specificity, positive predictive value and negative predictive value of whole-heart coronary MR angiography for detecting patients having significant stenosis were 82%, 90%, 88%, 86% [38], being higher than the results in our previous study using subject-specific acquisition windows exclusively in the diastolic phase.

A more recent multicenter study showed that non-contrast-enhanced whole-heart coronary MRA at 1.5 T with five-channel cardiac coils and a parallel imaging factor of 2 can detect significant CAD with high sensitivity (88%) and moderate specificity (72%). In particular, a negative predictive value of 88% indicates that whole-heart coronary MRA can effectively be used to rule out CAD [79]. Of note, the negative predictive value reported by this multicenter study is similar to the negative predictive value of the CORE-64 CTA multicenter study [6].

An introduction of 32-channel cardiac coils and a higher parallel imaging factor has considerably reduced the lengthy scan time as well as acquisition window and improved success rate of free-breathing whole-heart 3D coronary MR angiography. In a study by Nagata et al. that employed 32-channel cardiac coils, parallel imaging factor of 4, and abdominal belt technique, the sensitivity, specificity, positive predictive value, and negative predictive value of whole-heart coronary MRA at 1.5 T were 87%, 86%, 89%, and 83%, respectively, which was comparable to the diagnostic accuracy obtained by whole-heart coronary MRA using 5-channel coils but achieved those results in almost a half imaging time of whole-heart coronary MRA using 5-channel coils [32, 38] (Fig. 13.10).

Contrast-enhanced whole-heart coronary MRA at 3 T is a promising approach for a more accurate assessment of CAD. In a recent single-center study by Yang et al., 3 T MRA data were acquired with a gradient-echo sequence with inversion-recovery preparation during a slow infusion of double dose slightly albumin-binding contrast medium (gadopentetate dimeglumine; Multihance, Braco Imaging S.p.A, Milan, Italy) in consecutive 69 patient with suspected CAD. The sensitivity and specificity of 3 T whole-heart coronary MRA was 94% and 82%, respectively, for the detection of patients with >50% stenoses in the coronary arteries [80]. The same group recently conducted another single-center study by acquiring 3 T MRA data with 32-channel cardiac coils during a slow infusion of double

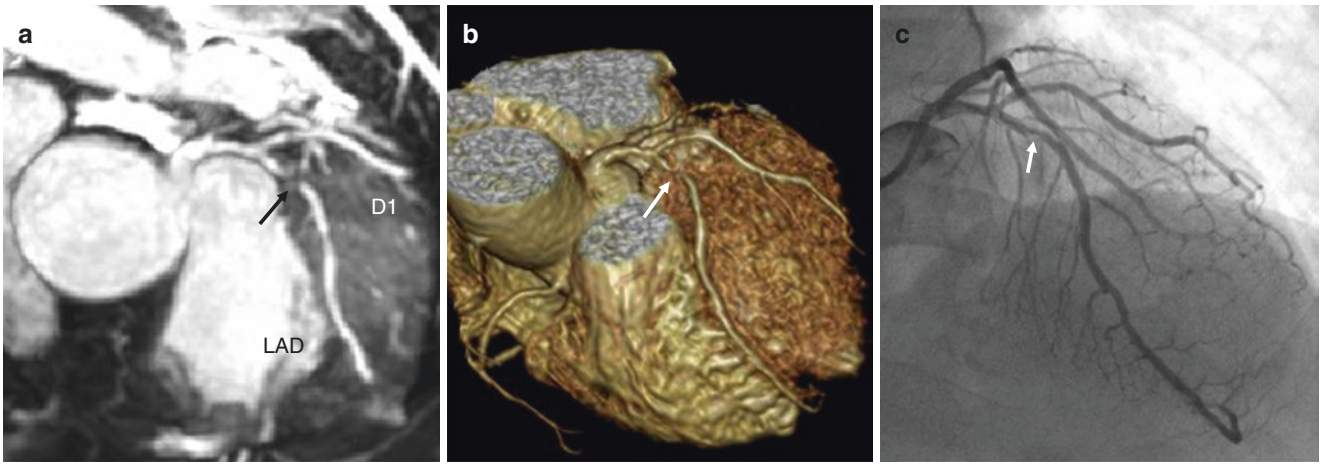

Fig. 13.10 A 50-year-old male patient with chest pain on effort. Significant stenosis in the proximal left anterior descending (LAD) thin SLAB maximum-intensity projection image (black arrow) (**a**), the volume-rendered image (white arrow) (**b**). The X-ray angiogram shows significant coronary artery stenosis in the proximal LAD (white arrow) (**c**) [32]. (Reprinted with permission from Nagata et al. [32], Copyright 2011, with permission from Radiological Society of North America)

dose same slightly albumin-binding contrast medium. Diagnostic quality MRA images were acquired in 101 of 110 (92%) patients with average imaging time of 7.0 ± 1.8 min [51]. The sensitivity, specificity, positive predictive value, and negative predictive value of 3 T contrast-enhanced whole-heart coronary MRA were 95.9%, 86.5%, 87.0%, and 95.7%, respectively, on a patient-based analysis, indicating that the diagnostic performance of 3 T contrast-enhanced whole-heart coronary MRA approaches to the diagnostic performance of 64-slice MDCT [6, 51]. Thus, whole-heart coronary MR angiography can be used as an alternative to coronary CT in ruling out significant coronary artery disease in patients with suspected coronary artery disease.

Diagnostic Accuracy of Quantitative Assessment of Whole-Heart Coronary MRA

Because of relatively limited spatial resolution of coronary MRA, accurate detection of the border of the coronary artery lumen and subsequent quantification of % stenosis is challenging. However, in contrast to coronary CTA, the signal intensity of the coronary arteries on MRA is little influenced by calcification of the coronary artery wall. By utilizing the insusceptibility to calcification, Yonezawa et al. [83] recently developed a method for quantitative analysis of stenosis on coronary MRA on the basis of the signal intensity profile along the vessel. The signal intensity profile along the vessel on 1.5 T whole-heart coronary MRA permits quantitative assessment of the severity of luminal narrowing in the coronary artery, with a sensitivity of 90% and a specificity of 80% in detecting >50% stenosis on X-ray coronary angiography. In addition, excellent agreement was observed between % stenoses determined by coronary MRA and X-ray coronary angiography, with a correlation coefficient of 0.84 ($P < 0.001$).

Additive Value of Whole-Heart Coronary MRA in a Comprehensive CMR Protocol

First-pass myocardial perfusion MRI with pharmacological stress allows for accurate assessment of myocardial ischemia caused by flow-limiting coronary artery disease (CAD) [84]. Since stress perfusion MRI can detect functional alteration of myocardial perfusion and coronary MRA can reveal morphological narrowing caused by atherosclerotic CAD, combined use of stress perfusion MRI and coronary MRA may be of important value in improving the diagnostic performance of CMR in detecting obstructive CAD. In a previous study by Klein et al. published in 2008 [85], however, the combination of coronary MRA and stress perfusion MRI failed to improve the diagnostic performance of stress perfusion MRI alone for the detection of stenosis >50% on invasive coronary angiography. In another study by Bettencourt et al. addition of whole-heart coronary MRA did not significantly improve the diagnostic accuracy of stress-rest myocardial perfusion and LGE MRI study for the detection of functionally significant coronary artery disease determined by invasive fractional flow reserve [86]. The sub-analysis of the recent multicenter prospective trial, CE-MARC study, also has concluded that the inclusion of coronary MRA provided no additional benefit when compared to the combination of stress perfusion, cine, and LGE CMR [87]. In CE-MARC study, however, the overall CMR result was judged positive if any CMR component was positive. This algorithm trends toward the overestimation of the grade of

coronary artery disease. Heer et al. applied a more differentiated algorithm, restricting coronary MRA integration to low confidence results of stress perfusion CMR and showed that combination of stress perfusion CMR and whole-heart coronary MRA in one comprehensive examination increases in specificity (from 79.3% to 88.9%) without worsening sensitivity (from 86.7% to 95.7%) [88].

Prognostic Performance of Whole-Heart Coronary MRA

An increasing number of studies demonstrated the prognostic value of coronary CTA for predicting the future cardiovascular events. However, the prognostic value of coronary MRA has not been investigated. A recent study by Yoon et al. evaluated the prognosis of 207 patients with suspected CAD who underwent 1.5 T whole-heart coronary MRA. They found that the presence of >50% stenosis on coronary MRA is strongly associated with the future cardiac death and major adverse cardiac events, indicating the value of whole-heart coronary MRA in predicting the future risk for cardiac events in patients with suspected CAD [89]. For example, the event-free survival for all cardiac events was 6.3% in patients with stenosis and 0.3% in those without stenosis ($P < 0.001$), indicating that the absence of significant stenosis on whole-heart coronary MRA is associated with a very low risk of cardiac events (Fig. 13.11).

Coronary MR Angiography vs. Coronary CT Angiography

Newer 64-slice CT imagers have a shorter rotation time and offer shorter scan time, higher spatial resolution (0.4 mm), and higher temporal resolution (165 ms) compared with previous generation CT scanners [5]. A recent study directly compared the diagnostic performances of 64-slice CT and volume-targeted coronary thin-slab FIESTA MR angiography [90]. High-resolution 3D FIESTA coronary MR angiography and coronary CT angiography demonstrated a similar accuracy in detecting proximal coronary stenosis. Compared to coronary angiography, sensitivity, specificity, and positive predictive value and negative predictive value for detecting >50% proximal coronary stenosis were 83.0%, 86.9%, 58.8%, and 96.5% for coronary MRA and 85.1%, 87.2%, 60.0%, and 95.6% for coronary CTA, respectively. For the 24 calcified stenoses, MRA correctly predicted the presence or absence of stenosis in 16 segments that were overestimated on CTA.

Despite the excellent diagnostic accuracy, coronary CT angiography has several non-negligible limitations. While estimated radiation dose during CT coronary has been substantially reduced over the past 10 years, radiation exposure to the patients is not negligible particularly in children and young adults. In addition, the diagnostic performance of

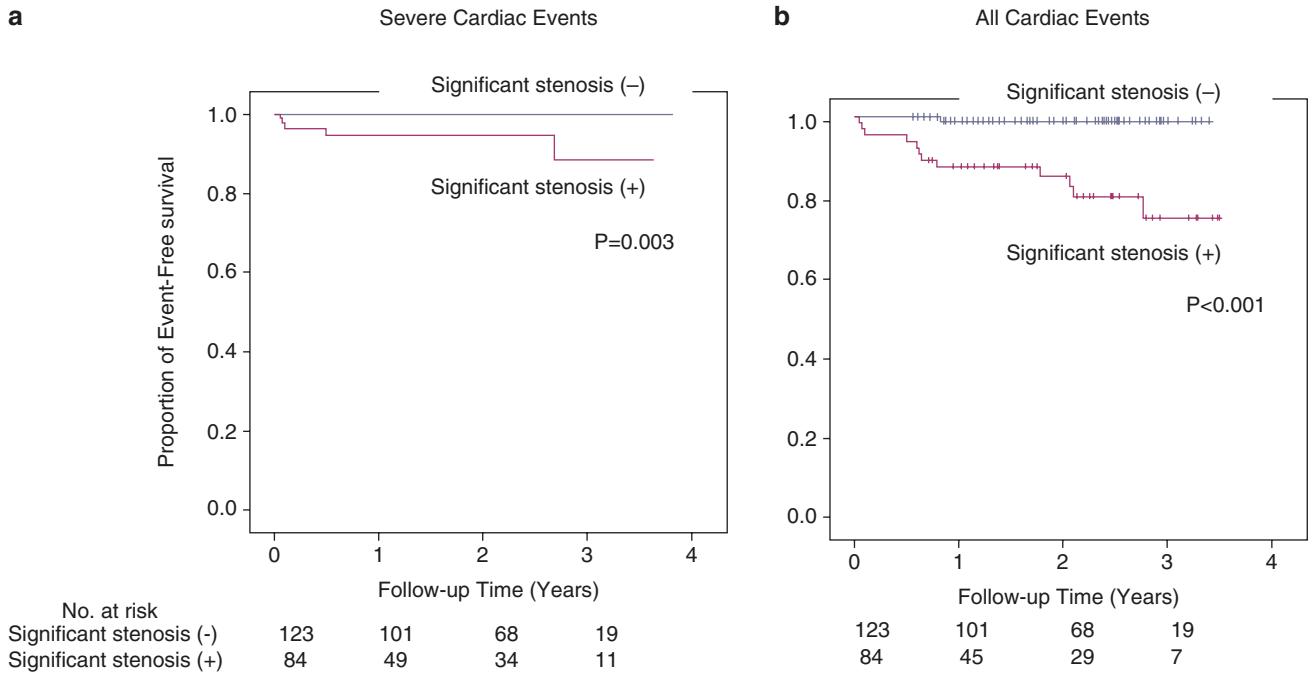

Fig. 13.11 Kaplan-Meier event-free survival curves for (**a**) severe cardiac events and (**b**) all cardiac events. The frequency of severe cardiac events as well as all cardiac events were significantly higher in patients with significant stenosis on whole-heart coronary MR angiography in comparison with patients without significant stenosis. The absence of significant stenosis on whole-heart coronary MR angiography can identify a population with a very low risk for severe cardiac events (0%) and al cardiac events (0.3%) during a median follow-up period [89]. (Reprinted from Yoon et al. [89], Copyright 2012, with permission from Elsevier)

coronary AT angiography is substantially impaired in patients with heavy coronary calcification. Coronary MR angiography and multi-slice coronary CT angiography are complement one another rather than to compete with one another, and coronary MR angiography seems to be useful in the following circumstances:

1. Coronary artery anomalies
2. Coronary artery aneurysm in patients with Kawasaki disease
3. Coronary arterial stenoses in patients with renal failure
4. Coronary arterial stenoses in patients with heavy calcification

Coronary MR angiography can successfully delineate anomalous coronary arteries and coronary artery aneurysms in Kawasaki disease without exposing the patients to radiation. Non-contrast-enhanced coronary MR angiography is well suited for assessing coronary artery disease in patients with renal failure. Coronary MR angiography is also useful in the visualization of coronary arterial lumen in patients with heavy coronary calcification (Fig. 13.12). Coronary MR angiography may have a role in screening coronary artery disease in asymptomatic subjects and those with relatively low likelihood of coronary artery disease, since coronary images can be obtained without exposing the subjects to ionizing radiation or administrating contrast medium. However, further study is required to determine the effectiveness of coronary MR angiography in screening coronary artery disease in the subjects with low prevalence of the disease, because false-positive cases may undergo unnecessary coronary CT angiography or invasive coronary angiography.

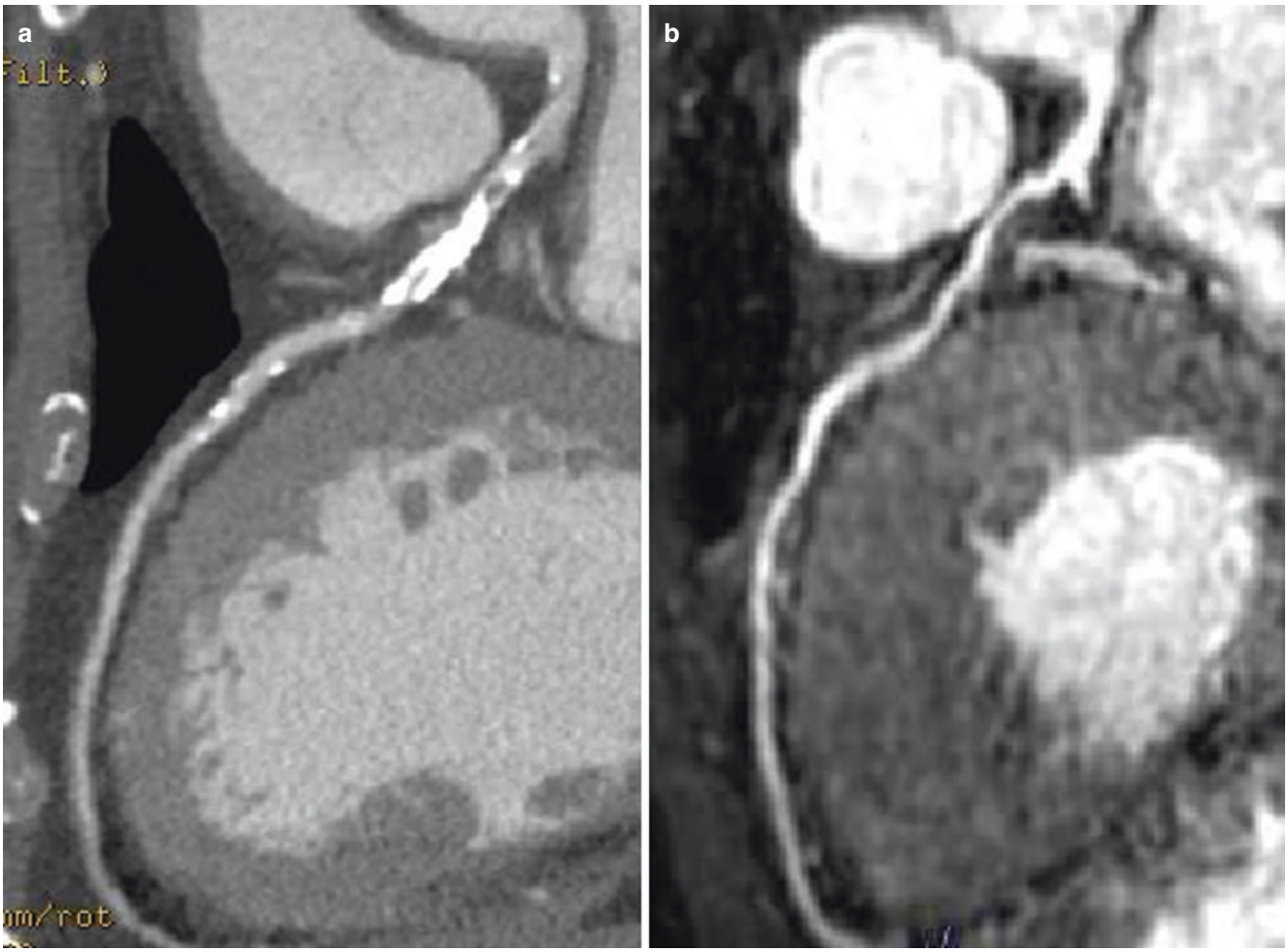

Fig. 13.12 Coronary CT angiography (64-slice VCT) and whole-heart coronary MR angiography in a 71-year-old man with anterior chest pain on effort. (**a**), Curved multi-planar reformatted image of 64-slice contrast-enhanced CT angiography demonstrates severely calcified plaque in the proximal left anterior descending artery. Luminal narrowing of the coronary artery cannot be assessed in this segment due to heavy coronary calcification. (**b**), Curved multi-planar reformatted image of non-contrast-enhanced whole-heart coronary MR angiography can clearly identify luminal narrowing in the proximal left anterior descending artery

Coronary Artery Wall Imaging

Non-contrast-Enhanced Approach

Several clinical studies demonstrated the ability of coronary artery wall imaging to assess coronary artery wall thickness and outward positive remodeling with relative lumen preservation using non-contrast CMR in patients with subclinical coronary artery disease [91, 92] and in patients with type 1 diabetes mellitus and in a multiethnic population cohort [93]. Additionally, Jansen et al. have demonstrated that non-contrast-enhanced T1-weighed (TIW) MRI allows direct thrombus visualization in patients with acute myocardial infarction [94]. Kawasaki et al. have previously shown that the presence of coronary high-intensity plaques (HIPs) detected by non-contrast T1W MRI is associated with positive coronary artery remodeling, low density on coronary CTA, and ultrasound attenuation [95]. Recently, Noguchi evaluated the relationship between HIPs and subsequent coronary events, demonstrating that HIPs identified by non-contrast-enhanced T1W MRI are significantly associated with coronary events and may be a promising predictive factor in patients [96]. In their study, the plaque-to-myocardium signal intensity ratio (PMR) was determined in each coronary plaque. Multivariate analysis showed that the presence of plaques with PMRs 1.4 is the significant independent predictor of coronary events (hazard ratio: 3.96; 95% confidence interval: 1.92–8.17; $p < 0.001$) compared with the presence of CAD (hazard ratio: 3.56; 95% confidence interval: 1.76–7.20; $p < 0.001$) and other traditional risk factors (Fig. 13.13). More recently, the same group

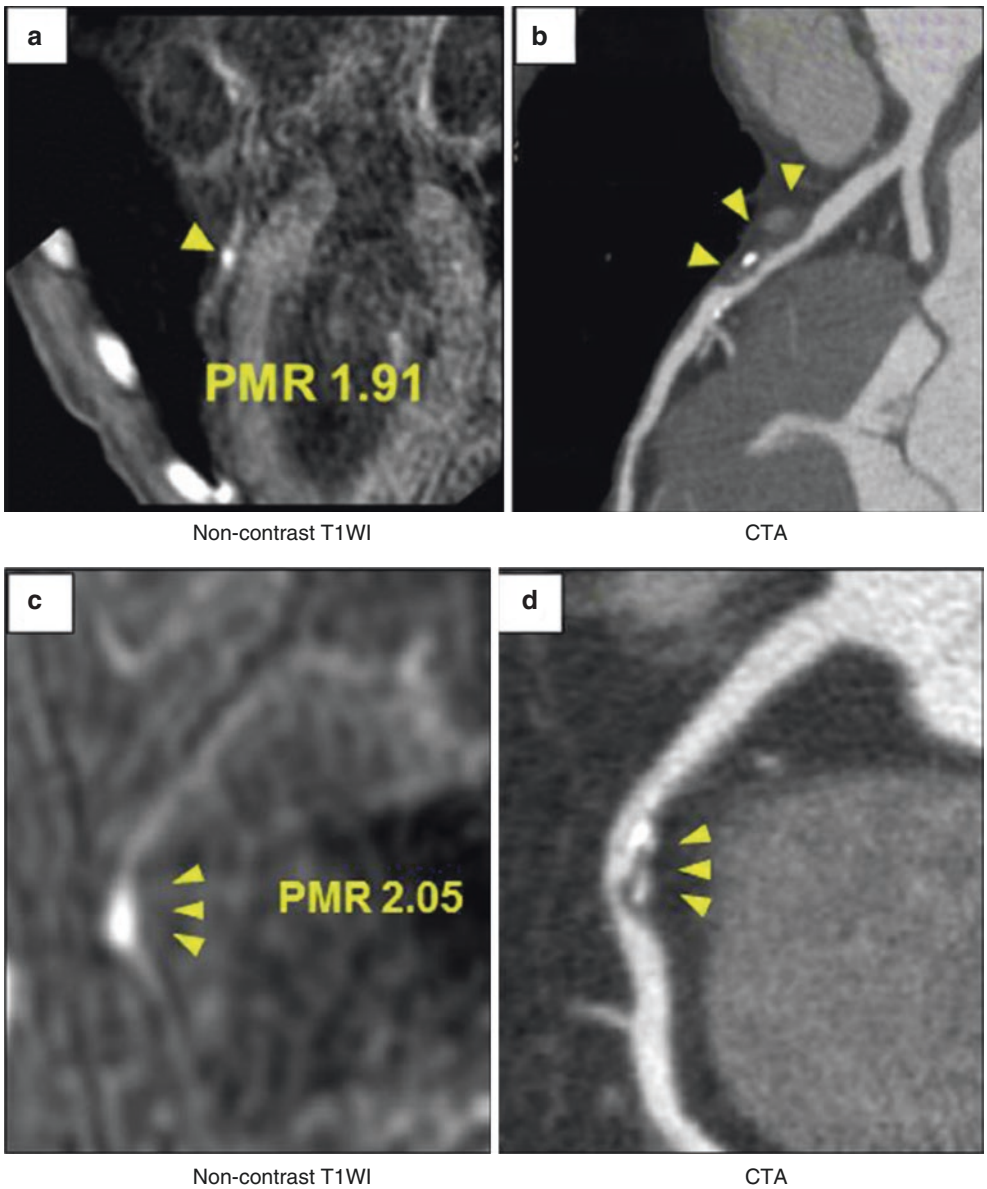

Fig. 13.13 Representative images of high-intensity plaques (HIP) on CMR. Representative non-contrast T1-weighted images of high-intensity plaques (HIPs) (yellow arrowheads) in the proximal left anterior descending coronary artery (**a**) and the right coronary artery (**c**), in which plaque-to-myocardium signal intensity ratios (PMRs) were 1.91 and 2.05, respectively. These high-intensity signals each correspond to the left and right coronary plaques on computed tomographic angiography (CTA) (yellow arrowheads on curved multi-planar reformation images, **b** and **d**) [96]. (Reprinted with permission from Noguchi et al. [96], © 2014, with permission from Elsevier)

investigated if intensive statin therapy can reduce the PMR of high-intensity plaques [97]. Non-contrast-enhanced T1W MRI was performed at baseline and after 12 months in 48 patients with coronary artery disease who underwent intensive statin treatment. In 48 control subjects with coronary artery disease who were not treated with statin, the PMR significantly increased (from 1.22 to 1.49, a 19.2% increase; $p < 0.001$). In contrast, 12 months of statin therapy significantly reduced the PMR (1.38–1.11, an 18.9% reduction; $p < 0.001$).

Contrast-Enhanced Approach

Coronary arterial wall contrast-enhanced CMR with MR contrast agent represents an alternative approach for the characterization of the atherosclerotic coronary arterial wall. Clinically approved MR contrast agents with extracellular distribution showed nonspecific uptake in coronary plaques both in patients with chronic angina [98] and in patients with acute coronary syndromes [99]. In patients with stable angina, gadolinium contrast enhancement in the coronary arterial wall is associated with calcified or mixed plaques on MSCT, while patients with ACS exhibited transit contrast uptake. These studies demonstrated that contrast agent uptake in the coronary artery wall could be associated with both atherosclerotic plaque composition and inflammation.

Several novel target-specific contrast agents have been developed and tested in animal models. Currently, two targeted contrast agents are approved for human use: (1) an albumin-binding contrast agent (gadofosveset trisodium; Lantheus Medical Imaging, North Billerica, MA) and (2) iron oxide-based contrast agent (ferumoxytol; Advanced Magnetics Inc., Cambridge, MA). Albumin-binding contrast agent has been developed for MR angiography of the large and coronary vessels. The accumulation of albumin-binding contrast agent in the coronary arterial wall is associated with increased endothelial permeability and/or increased neovascularization [100, 101]. Furthermore, iron oxide-based contrast agent (USPIO) also has been shown to be useful for the imaging of inflammatory cell infiltration after myocardial infarction [102, 103], and enhancement by USPIO is associated with increased endothelial permeability of the vessel wall.

Future Perspectives

Despite the recent advance of hardware and software of clinical MR system, several limitations still remain for coronary MRA such as long scan times, limited spatial resolution, and SNR compared to coronary CTA. To overcome these limitations, direct respiratory motion estimation techniques of the heart and compressed sensing techniques have been intensively investigated in the recent several years in addition to the abovementioned variety of the techniques. Although those recent technical advancements have not yet been applied to routine clinical practices, these new technologies may substantially expand the use of MR coronary imaging in patients with coronary artery disease in the future.

Sophisticated Respiratory Motion Compensation Technique

Free-breathing coronary MRA with conventional one-dimensional respiratory navigator uses a simplified model for respiratory motion correction, typically with a fixed correction factor of 0.6, which accounts for respiratory-induced superior-inferior (SI) translational motion of the heart only [34]. This simple linear model cannot fully compensate the bulk respiratory-induced heart motion. Therefore, respiratory gating with 1D navigator echoes considerably reduce motion artifact only when narrow respiratory gating windows are employed. However, it leads to prolonged scan time since only a fraction of the acquired data is accepted for reconstruction. Recently, several approaches have been proposed to overcome some of these problems such as (1) self-gating technique [104–107], (2) image-based navigation techniques [108–110], and "respiratory binning" techniques with 3D affine motion correction [111–114] (Fig. 13.14).

Self-Gating Technique

With self-gating, information about the respiratory displacement of the heart is directly extracted from the very same data used for imaging. Furthermore, the placement of the navigator is no longer necessary and no delay between motion detection and data acquisition has to be account for. Scan efficiency increases to 100% as all data segments are used for the final image reconstruction [104, 105]. In this approach, typically a 1D projection image of the heart is acquired in superior-inferior (SI) direction. One of these SI projections is taken as reference. Then, the relative displacement between the position of the heart in each acquired projection and the references is determined and corrected. One study reported that the use of end-expiration as a respiratory reference position is the most promising in terms of image quality on self-navigation coronary MRA in healthy adult subjects [106]. However, in case of more irregular respiration and respiratory drift as often occurring in patients, this may no longer be correct, and alternative strategies may be needed. Ginami et al. developed an iterative self-navigator technique that no longer depends on the choice of a specific respiratory reference position [107].

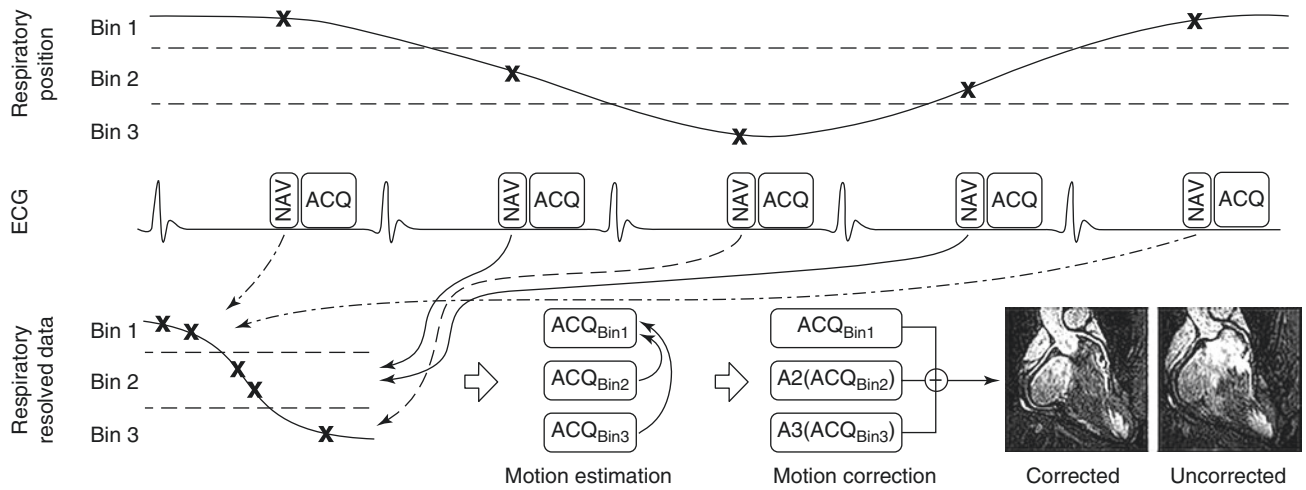

Fig. 13.14 Schematic of a general respiratory binning, motion estimation, and correction procedure. The respiratory position is measured using a navigator (NAV) for each k-space acquisition (ACQ) and allocated to a respiratory bin. Respiratory resolved data from each bin can be reconstructed separately (ACQ_{Bin1-3}) although undersampled. For non-Cartesian k-space sampling the undersampled data from each bin can be used to estimate motion between bins. However, additional fully sampled navigator data is necessary for Cartesian k-space sampling. The respiratory motion is typically estimated by registering ACQ_{Bin2} and ACQ_{Bin3} to the end-expiratory ACQ_{Bin1} to generate the transformations A_2 and A_3. The motion corrected CMRA data can be obtained by applying these transformations to the CMRA data in the corresponding bins and summing the results. Note, in this example 3 respiratory bins are used; however, in practice 4–6 bins are typically employed. (Image courtesy of Dr. Markus Henningsson, Kings College London, UK)

Image-Based Navigation Techniques

Image-based navigation techniques commonly use 2D or 3D image navigators [108–110]. Most of these image-based approaches correct respiratory motion in a beat-to-beat fashion. Henningsson et al. developed a 2D navigator to allow for prospective correction of translational motion of the heart in two directions [108, 109]. In this method the startup pulse of SSFP have been used to spatially encode a low-resolution image immediately before the acquisition of k-space data. The respiratory-induced heart motion is estimated along the SI and RL directions using the low-resolution 2D images and is used to correct the high-resolution data. This implementation of 2D navigator allows for increased scan efficiency without comprising image quality and more flexibility to separately determine the imaging and navigator parameters. More recently, Moghari et al. proposed 3D heart locator technique for whole-heart coronary MR angiography, which is a 3D version of image-based navigation techniques [110].

"Respiratory Binning" Techniques with 3D Affine Motion Correction

To account for more complex and 3D motion, "respiratory binning" techniques with 3D affine motion correction have been recently proposed [111–114]. With this approach the respiratory signal is divided into several states of the breathing cycle or "bins" and afterward corrected to a reference position using the motion estimated from low-resolution images [111]. These methods achieve 100% scan efficiency and therefore reduce the acquisition time. Several investigators have recently applied 3D affine motion correction scheme to self-gating and image-based navigations [112–114]. Pang J et al. have developed an improved respiratory motion correction scheme with 3D self-navigation and image-based affine motion correction [112], reducing the imaging time to 7.1 ± 0.5 min from 13.9 ± 2.6 min with conventional navigator gating. Aitken et al. combined "beat-to-beat" translational motion correction using 2D navigator with "bin-to-bin" affine motion correction for 3D whole-heart coronary MR angiography [113]. Those above-mentioned studies employed radial k-space trajectories. SENSE has been proven effective for non-Cartesian trajectories and is usually accomplished by inverting the encoding matrix using iterative methods such as conjugated-gradients (iterative SENSE) [114]. As the self-navigation utilizes non-Cartesian trajectories, k-space central region for the self-navigation is oversampled and can be used to reconstruct alias-free low-resolution images for the estimation of sensitivity map without the need for extra scan. Consequently, Pang et al. combined 3D self-navigation scheme with self-calibrating iterative SENSE reconstruction, demonstrating that this combined method significantly improves the image quality compared with self-navigation with an image-based 3D-affine motion correction only [111]. However, the radial k-space trajectories have intrinsically lower SNR compared to Cartesian trajectories. Henningsson et al. recently proposed the 3D affine motion correction for Cartesian whole-heart coronary MR

angiography using a 3D image-based navigator to allow for data acquisition throughout the whole respiratory cycle and demonstrated that this technique can be used to acquire Cartesian whole-heart 3D coronary artery images with 100% scan efficiency with similar image quality as compared with the state-of-the-art-gated and corrected method with approximately 50% scan efficiency [115].

Compressed Sensing and Iterative K-Space Reconstruction

Compressed sensing (CS) is a new image reconstruction method for accelerated acquisitions with incoherently undersampled k-space data, which can be achieved by random undersampling in the ky–kz plane for 3D Cartesian acquisitions by exploiting the sparsity of the image in a transform domain [116]. Recently, a CS-based reconstruction strategy for high-resolution CMR, called low-dimensional-structure self-learning and thresholding (LOST), has been developed, providing reconstructions with reduced blurring compared to conventional CS techniques [117]. This CS technique was successfully utilized in non-contrast- and contrast-enhanced whole-heart coronary MRI [118]. Then, Akcakaya et al. employed this CS technique for highly accelerated submillimeter whole-heart coronary MRA and performed a head-to-head comparison of such CS techniques utilizing prospective random k-space undersampling versus parallel imaging with prospective uniform undersampling [119]. They demonstrated that the image quality and SNR of the CS images were significantly higher than those of coronary MA images accelerated by parallel imaging [119].

CS can be also utilized for the respiratory motion compensation by estimating the motion-corrupted k-space data without reacquiring k-space data [120], because the quasiperiodic nature of the respiratory pattern yields a randomly undersampled k-space in CMR. Moghari et al. proposed a joint prospective-retrospective navigator echo motion compensation algorithm. In this technique, the inner k-space region is acquired using a prospective navigator, while, for the outer k-space, a navigator is only used to reject the motion-corrupted data without reacquiring them. Subsequently, those unfilled k-space lines are retrospectively estimated using compressed sensing reconstruction [120]. This approach yields a scan time reduction in coronary MRI, maintaining subjective and objective image quality of coronary MRA [121].

Forman et al. employed a different approach, which combined weighted iterative reconstruction technique with self-navigated free-breathing coronary MRA for retrospective reduction of respiratory motion artifact. They found that total imaging time was reduced with sufficient suppression of respiratory motion artifacts [121].

Four-Dimensional Whole-Heart MR Imaging

While prospective acquisition is commonly used for coronary MRA, a retrospective navigator gating is also possible and useful for improved gating efficiency or completion of scan in a fixed amount of time. Cardiac cine MR imaging commonly employs retrospective ECG gating to address cardiac motion. When data acquisition is performed continuously in a free running mode with retrospective ECG gating in combination with retrospective respiratory self-gating, 4D whole-heart imaging can be achieved. Coppo et al. have developed a free running 4D whole-heart self-navigated coronary MR imaging using golden angle k-space filling, enabling the assessment of both coronary anatomy and ventricular function simultaneously, with retrospective and flexible acquisition window selection for the best visualization of each coronary segment [122]. Furthermore, as cardiac phase information also can be obtained by cardiac self-gating, compensation of both cardiac and respiratory motion also enables 4D coronary MR imaging. Pang et al. have developed a free-breathing and free running 4D coronary MRA technique with simultaneously cardiac and respiratory self-gating, golden angle 3D radial k-space sampling, and feasibility of isotropic whole-heart MR imaging has been demonstrated [123].

References

1. Writing Group Memebers. Heart disease and stroke statistics—2015 update a report from the American Heart Association. Circulation. 2015;131:e29–e322.
2. Scanlon PJ, Faxon DP, Audet AM, et al. ACC/AHA guidelines for coronary angiography. A report of the American College of Cardiology/American Heart Association Task Force on practice guidelines (Committee on Coronary Angiography). Developed in collaboration with the Society for Cardiac Angiography and Interventions. J Am Coll Cardiol. 1999;33:1756–824.
3. Budoff MJ, Georgiou D, Brody A, et al. Ultrafast computed tomography as a diagnostic modality in the detection of coronary artery disease: a multicenter study. Circulation. 1996;93:898–904.
4. Raff GL, Gallagher MJ, O'Neill WW, Goldstein JA. Diagnostic accuracy of noninvasive coronary angiography using 64-slice spiral computed tomography. J Am Coll Cardiol. 2005;46:552–7.
5. Mollet NR, Cademartiri F, van Mieghem CA, Runza G, McFadden EP, Baks T, et al. High-resolution spiral computed tomography coronary angiography in patients referred for diagnostic conventional coronary angiography. Circulation. 2005;112:2318–23.
6. Miller JM, Rochitte CE, Dewey M, Arbab-Zadeh A, Niinuma H, Gottlieb I, et al. Diagnostic performance of coronary angiography by 64-row ct. N Engl J Med. 2008;359:2324–36.
7. Budoff MJ, Dowe D, Jollis JG, Gitter M, Sutherland J, Halamert E, et al. Diagnostic performance of 64-multidetector row coronary computed tomographic angiography for evaluation of coronary artery stenosis in individuals without known coronary artery disease: results from the prospective multicenter ACCURACY (Assessment by Coronary Computed Tomographic Angiography of Individuals Undergoing Invasive Coronary Angiography) trial. J Am Coll Cardiol. 2008;52:1724–32.

8. Chinnaiyan KM, Boura JA, DePetris A, Gentry R, Abidov A, Share DA, et al. Progressive radiation dose reduction from coronary computed tomography angiography in a statewide collaborative quality improvement program: results from the Advanced Cardiovascular Imaging Consortium. Circ Cardiovasc Imaging. 2013;6:646–54.
9. Edelman RR, Manning WJ, Pearlman J, Li W. Human coronary arteries: projection angiograms reconstructed from breath-hold two-dimensional MR images. Radiology. 1993;187:719–22.
10. Manning WJ, Li W, Edelman RR. A preliminary report comparing magnetic resonance coronary angiography with conventional angiography. N Eng J Med. 1993;328:828–32.
11. Sakuma H, Caputo GR, Steffens JC, O'Sullivan M, Bourne MW, Shimakawa A, et al. Breath-hold MR cine angiography of coronary arteries in healthy volunteers: value of multiangle oblique imaging planes. Am J Roentgenol. 1994;163:533–7.
12. Wielopolski PA, Manning WJ, Edelman RR. Single breath-hold volumetric imaging of the heart using magnetization-prepared 3-dimensional segmented echo planar imaging. J Magn Reson Imaging. 1995;5:403–9.
13. Bornert P, Jensen D. Coronary artery imaging at 0.5 T using segmented 3D echo planar imaging. Magn Reson Med. 1995;34:779–85.
14. Wielopolski PA, van Geuns RJ, de Feyter PJ, Oudkerk M. Breath-hold coronary MR angiography with volume-targeted imaging. Radiology. 1998;209:209–129.
15. van Geuns RJ, Wielopolski PA, de Bruin HG, Rensing BJ, Hulshoff M, van Ooijen PM, et al. MR coronary angiography with breath-hold targeted volumes: preliminary clinical results. Radiology. 2000;217:270–27.
16. Foo TK, Ho VB, Saranathan M, Cheng LQ, Sakuma H, Kraitchman DL, et al. Feasibility of integrating high-spatial-resolution 3D breath-hold coronary MR angiography with myocardial perfusion and viability examinations. Radiology. 2005;235:1025–30.
17. Goldfarb JW, Edelman RR. Coronary arteries: breath-hold, adolinium-enhanced, three-dimensional MR angiography. Radiology. 1998;206:830–4.
18. Kessler W, Laub G, Achenbach S, Ropers D, Moshage W, Daniel WG. Coronary arteries: MR angiography with fast contrast-enhanced three-dimensional breath-hold imaging–initial experience. Radiology. 1999;210:566–72.
19. Li D, Carr JC, Shea SM, Zheng J, Deshpande VS, et al. Coronary arteries: magnetization-prepared contrast-enhanced three-dimensional volume-targeted breath-hold MR angiography. Radiology. 2001;219:270–7.
20. Regenfus M, Ropers D, Achenbach S, Kessler W, Laub G, et al. Noninvasive detection of coronary artery stenosis using contrast-enhanced three-dimensional breath-hold magnetic resonance coronary angiography. J Am Coll Cardiol. 2000;36:44–50.
21. Holland AE, Goldfarb JW, Edelman RR. Diaphragmatic and cardiac motion during suspended breathing: preliminary experience and implications for breath-hold MR imaging. Radiology. 1998;209:483–9.
22. Oshinski JN, Hofland L, Mukundan S Jr, Dixon WT, Parks WJ, Pettigrew RI. Two-dimensional coronary MR angiography without breath holding. Radiology. 1996;201:737–43.
23. McConnell MV, Khasgiwala VC, Savord BJ, Chen MH, Chuang ML, et al. Comparison of respiratory suppression methods and navigator locations for MR coronary angiography. Am J Roentgenol. 1997;168:1369–75.
24. Li D, Kaushikkar S, Haacke EM, et al. Coronary arteries: three-dimensional MR imaging with retrospective respiratory gating. Radiology. 1996;201:857–63.
25. Post JC, van Rossum AC, Hofman MB, Valk J, Visser CA. Three-dimensional respiratory-gated MR angiography of coronary arteries: comparison with conventional coronary angiography. Am J Roentgenol. 1996;166:1399–404.
26. Woodard PK, Li D, Haacke EM, Dhawale PJ, Kaushikkar S, Barzilai B, et al. Detection of coronary stenoses on source and projection images using three-dimensional MR angiography with retrospective respiratory gating: preliminary experience. Am J Roentgenol. 1998;170:883–8.
27. Stuber M, Botnar RM, Danias PG, Kissinger KV, Manning WJ. Submillimeter three-dimensional coronary MR angiography with real-time navigator correction: comparison of navigator locations. Radiology. 1999;212:579–87.
28. Botnar RM, Stuber M, Danias PG, Kissinger KV, Manning WJ. Improved coronary artery definition with T2-weighted, free-breathing, three-dimensional coronary MRA. Circulation. 1999;99:3139–48.
29. Stuber M, Botnar RM, Danias PG, Sodickson DK, Kissinger KV, Van Cauteren M, et al. Double-oblique free-breathing high resolution three-dimensional coronary magnetic resonance angiography. J Am Coll Cardiol. 1999;34:524–31.
30. Kim WY, Danias PG, Stuber M, Flamm SD, Plein S, Nagel E, et al. Coronary magnetic resonance angiography for the detection of coronary stenoses. N Eng J Med. 2001;345:1863–9.
31. Nagel E, Bornstedt A, Schnackenburg B, Hug J, Oswald H, Fleck E. Optimization of realtime adaptive navigator correction for 3D magnetic resonance coronary angiography. Magn Reson Med. 1999;42:408–11.
32. Nagata M, Kato S, Kitagawa K, et al. Diagnostic accuracy of 1.5-T unenhanced whole-heart coronary MR angiography performed with 32-channel cardiac coils: initial single-center experience. Radiology. 2011;259:384–92.
33. Ishida M, Schuster A, Takase S, et al. Impact of an abdominal belt on breathing patterns and scan efficiency in whole-heart coronary magnetic resonance angiography: comparison between the UK and Japan. J Cardiovasc Magn Reson. 2011;13:71–81.
34. Stuber M, Botnar RM, Danias PG, Kissinger KV, Manning WJ. Submillimeter 3D coronary MRA using real-time navigator correction: comparison of navigator locations. Radiology. 1999;212:579–87.
35. Wang Y, Vidan E, Bergman GW. Cardiac motion of coronary arteries: variability in the rest period and implications for coronary MR angiography. Radiology. 1999;213:751–8.
36. Kim WY, Stuber M, Kissinger KV, Andersen NT, Manning WJ, Botnar RM. Impact of bulk cardiac motion on right coronary MR angiography and vessel wall imaging. J Magn Reson Imaging. 2001;14:383–90.
37. Plein S, Jones TR, Ridgway JP, Sivananthan MU. Three-dimensional coronary MR angiography performed with subject-specific cardiac acquisition windows and motion-adapted respiratory gating. Am J Roentgenol. 2003;180:505–12.
38. Sakuma H, Ichikawa Y, Chino S, Hirano T, Makino K, Takeda K. Detection of coronary artery stenosis with whole-heart coronary magnetic resonance angiography. J Am Coll Cardiol. 2006;48:1946–50.
39. Carr JC, Simonetti O, Bundy J, Li D, Pereles S, Finn JP. Cine MR angiography of the heart with segmented true fast imaging with steady-state precession. Radiology. 2001;219:828–34.
40. McCarthy RM, Shea SM, Deshpande VS, Green JD, Pereles FS, Carr JC, et al. Coronary MR angiography: true FISP imaging improved by prolonging breath holds with preoxygenation in healthy volunteers. Radiology. 2003;227:283–8.
41. Spuentrup E, Katoh M, Buecker A, Manning WJ, Schaeffter T, Nguyen TH, et al. Free-breathing 3D steady-state free precession coronary MR angiography with radial k-space sampling: comparison with cartesian k-space sampling and cartesian gradient-echo coronary MR angiography – pilot study. Radiology. 2004;231:581–6.
42. Weber OM, Martin AJ, Higgins CB. Whole-heart steady-state free precession coronary artery magnetic resonance angiography. Magn Reson Med. 2003;50:1223–8.

43. Sakuma H, Ichikawa Y, Suzawa N, Hirano T, Makino K, Koyama N, et al. Assessment of coronary arteries with total study time of less than 30 minutes by using whole-heart coronary MR angiography. Radiology. 2005;237:316–21.
44. Stuber M, Botnar RM, Fischer SE, et al. Preliminary report on in vivo coronary MRA at 3 Tesla in humans. Magn Reson Med. 2002;48:425–9.
45. Sommer T, Hackenbroch M, Hofer U, Schmiedel A, Willinek WA, Flacke S, et al. Coronary MR angiography at 3.0 T versus that at 1.5 T: initial results in patients suspected of having coronary artery disease. Radiology. 2005;234:718–25.
46. Kaul MG, Stork A, Bansmann PM, et al. Evaluation of balanced steady-state free precession (TrueFISP) and K-space segmented gradient echo sequences for 3D coronary MR angiography with navigator gating at 3 Tesla. Rofo. 2004;176:1560–5.
47. Soleimanifard S, Schär M, Hays AG, Prince JL, Weiss RG, Stuber M. Spatially selective implementation of the adiabatic T2Prep sequence for magnetic resonance angiography of the coronary arteries. Magn Reson Med. 2013;70:97–105.
48. Li D, Paschal CB, Haacke EM, Adler LP. Coronary arteries: three-dimensional MR imaging with fat saturation and magnetization transfer contrast. Radiology. 1993;187:401–6.
49. Börnert P, Koken P, Nehrke K, Eggers H, Ostendorf P. Water/fat-resolved whole-heart Dixon coronary MRA: an initial comparison. Magn Reson Med. 2014;71:156–63.
50. Tang L, Merkle N, Schär M, et al. Volume-targeted and whole-heart coronary magnetic resonance angiography using an intravascular contrast agent. J Magn Reson Imaging. 2009;30:1191–6.
51. Yang Q, Li K, Liu X, et al. Contrast-enhanced whole-heart coronary magnetic resonance angiography at 3.0-T: a comparative study with X-ray angiography in a single center. J Am Coll Cardiol. 2009;54:69–76.
52. Reimer P, Bremer C, Allkemper T, Engelhardt M, Mahler M, et al. Myocardial perfusion and MR angiography of chest with SH U 555 C: results of placebo-controlled clinical phase i study. Radiology. 2004;231:474–81.
53. Klein C, Schalla S, Schnackenburg B, Bornstedt A, Hoffmann V, et al. Improvement of image quality of non-invasive coronary artery imaging with magnetic resonance by the use of the intravascular contrast agent Clariscan (NC100150 injection) in patients with coronary artery disease. J Magn Reson Imaging. 2003;17:656–62.
54. Stuber M, Botnar RM, Danias PG, McConnell MV, Kissinger KV, Yucel EK, Manning WJ. Contrast agent-enhanced, free-breathing, three-dimensional coronary magnetic resonance angiography. J Magn Reson Imaging. 1999;10:790–9.
55. Paetsch I, Huber ME, Bornstedt A, Schnackenburg B, Boesiger P, Stuber M, et al. Improved three-dimensional free-breathing coronary magnetic resonance angiography using gadocoletic acid (B-22956) for intravascular contrast enhancement. J Magn Reson Imaging. 2004;20:288–93.
56. Herborn CU, Barkhausen J, Paetsch I, Hunold P, Mahler M, et al. Coronary arteries: contrast-enhanced MR imaging with SH L 643A – experience in 12 volunteers. Radiology. 2003;229:217–23.
57. Laurent S, Elst LV, Muller RN. Comparative study of the physicochemical properties of six clinical low molecular weight gadolinium contrast agents. Contrast Media Mol Imaging. 2006;1:128–37.
58. Krombach GA, Hahnen C, Lodemann KP, et al. Gd-BOPTA for assessment of myocardial viability on MRI: changes of T1 value and their impact on delayed enhancement. Eur Radiol. 2009;19:2136–46.
59. Raman FS, Nacif MS, Cater G, Gai N, Jones J, Li D, et al. 3.0-T whole-heart coronary magnetic resonance angiography: comparison of gadobenate dimeglumine and gadofosveset trisodium. Int J Cardiovasc Imaging. 2013;29:1085–94.
60. Pruessmann KP, Weiger M, Scheidegger MB, Boesiger P. SENSE: sensitivity encoding for fast MRI. Magn Reson Med. 1999;42:952–62.
61. Griswold MA, Jakob PM, Heidemann RM, Nittka M, Jellus V, Wang J, et al. Generalized autocalibrating partially parallel acquisitions (GRAPPA). Magn Reson Med. 2002;47:1202–10.
62. Sodickson DK, Manning WJ. Simultaneous acquisition of spatial harmonics (SMASH): fast imaging with radiofrequency coil arrays. Magn Reson Med. 1997;38:591–603.
63. Reeder SB, Wintersperger BJ, Dietrich O, Lanz T, Greiser A, Reiser MF, et al. Practical approaches to the evaluation of signal-to-noise ratio performance with parallel imaging: application with cardiac imaging and a 32-channel cardiac coil. Magn Reson Med. 2005;54:748–54.
64. Gharib AM, Abd-Elmoniem KZ, Ho VB, Födi E, Herzka DA, Ohayon J, et al. The feasibility of 350 μm spatial resolution coronary magnetic resonance angiography at 3 T in humans. Invest Radiol. 2012;47:339–45.
65. Donaldson RM, Raphael MJ, Yacoub MH, Ross DN. Hemodynamically significant anomalies of the coronary arteries: surgical aspects. Thorac Cardiovasc Surg. 1982;30:7–13.
66. Click RL, Holmes DR Jr, Vlietstra RE, Kosinski AS, Kronmal RA. Anomalous coronary arteries: location, degree of atherosclerosis and effect on survival: a report from the Coronary Artery Surgery Study. J Am Coll Cardiol. 1989;13:531–7.
67. McConnell MV, Ganz P, Selwyn AP, Edelman RR, Manning WJ. Identification of anomalous coronary arteries and their anatomic course by magnetic resonance coronary angiography. Circulation. 1995;92:3158–62.
68. Taylor AM, Thorne SA, Rubens MB, Jhooti P, Keegan J, Gatehouse PD, et al. Coronary artery imaging in grown up congenital heart disease: complementary role of magnetic resonance and x-ray coronary angiography. Circulation. 2000;101:1670–8.
69. Bunce NH, Lorenz CH, Keegan J, Lesser J, Reyes EM, et al. Coronary artery anomalies: assessment with free-breathing three-dimensional coronary MR angiography. Radiology. 2003;227:201–8.
70. Datta J, White CS, Gilkeson RC, Meyer CA, Kansal S, Jani ML, et al. Anomalous coronary arteries in adults: depiction at multidetector row CT angiography. Radiology. 2005;235:812–8.
71. Kato H, Sugimura T, Akagi T, Sato N, Hashino K, Maeno Y, et al. Long-term consequences of Kawasaki disease. A 10- to 21-year follow-up study of 594 patients. Circulation. 1996;94:1379–85.
72. Greil GF, Stuber M, Botnar RM, Kissinger KV, Geva T, Newburger JW, et al. Coronary magnetic resonance angiography in adolescents and young adults with Kawasaki disease. Circulation. 2002;105:908–11.
73. Mavrogeni S, Papadopoulos G, Douskou M, Kaklis S, Seimenis I, Baras P, et al. Magnetic resonance angiography is equivalent to X-ray coronary angiography for the evaluation of coronary arteries in Kawasaki disease. J Am Coll Cardiol. 2004;43:649–52.
74. Duerinckx AJ, Urman MK. Two-dimensional coronary MR angiography: analysis of initial clinical results. Radiology. 1994;193:731–8.
75. Sandstede JJ, Pabst T, Beer M, Geis N, Kenn W, et al. Three-dimensional MR coronary angiography using the navigator technique compared with conventional coronary angiography. Am J Roentgenol. 1999;172:135–9.
76. Sardanelli F, Molinari G, Zandrino F, Balbi M. Three-dimensional, navigator-echo MR coronary angiography in detecting stenoses of the major epicardial vessels, with conventional coronary angiography as the standard of reference. Radiology. 2000;214:808–14.
77. Bogaert J, Kuzo R, Dymarkowski S, Beckers R, Piessens J, Rademakers FE. Coronary artery imaging with real-time navigator three-dimensional turbo-field-echo MR coronary angiography: initial experience. Radiology. 2003;226:707–16.

78. Kefer J, Coche E, Legros G, Pasquet A, Grandin C, Van Beers BE, et al. Head-to-head comparison of three-dimensional navigator-gated magnetic resonance imaging and 16-slice computed tomography to detect coronary artery stenosis in patients. J Am Coll Cardiol. 2005;46:92–100.
79. Kato S, Kitagawa K, Ishida N, Ishida M, Nagata M, Ichikawa Y, et al. Assessment of coronary artery disease using magnetic resonance coronary angiography: A national multicenter trial. J Am Coll Cardiol. 2010;56:983–91.
80. Yang Q, Li K, Liu X, Du X, Bi X, Huang F, et al. 3.0 T whole-heart coronary magnetic resonance angiography performed with 32-channel cardiac coils: a single-center experience. Circ Cardiovasc Imaging. 2012;5:573–9.
81. Jahnke C, Paetsch I, Schnackenburg B, Bornstedt A, Gebker R, et al. Coronary MR angiography with steady-state free precession: individually adapted breath-hold technique versus free-breathing technique. Radiology. 2004;232:669–76.
82. Jahnke C, Paetsch I, Nehrke K, Schnackenburg B, Gebker R, et al. Rapid and complete coronary arterial tree visualization with magnetic resonance imaging: feasibility and diagnostic performance. Eur Heart J. 2005;26:2313–9.
83. Yonezawa M, Nagata M, Kitagawa K, Kato S, Yoon Y, Nakajima H, et al. Quantitative analysis of 1.5-T whole-heart coronary MR angiograms obtained with 32-channel cardiac coils: a comparison with conventional quantitative coronary angiography. Radiology. 2014;271:356–64.
84. Jaarsma C, Leiner T, Bekkers SC, Crijns HJ, Wildberger JE, Nagel E, et al. Diagnostic performance of noninvasive myocardial perfusion imaging using single-photon emission computed tomography, cardiac magnetic resonance, and positron emission tomography imaging for the detection of obstructive coronary artery disease: a meta-analysis. J Am Coll Cardiol. 2012;59:1719–28.
85. Klein C, Gebker R, Kokocinski T, et al. Combined magnetic resonance coronary artery imaging, myocardial perfusion and late gadolinium enhancement in patients with suspected coronary artery disease. J Cardiovasc Magn Res. 2008;10:45–54.
86. Bettencourt N, Ferreira N, Chiribiri A, Schuster A, Sampaio F, Santos L, et al. Additive value of magnetic resonance coronary angiography in a comprehensive cardiac magnetic resonance stress-rest protocol for detection of functionally significant coronary artery disease: a pilot study. Circ Cardiovasc Imaging. 2013;6:730–8.
87. Ripley DP, Motwani M, Brown JM, Nixon J, Everett CC, Bijsterveld P, et al. Individual component analysis of the multiparametric cardiovascular magnetic resonance protocol in the CE-MARC trial. J Cardiovasc Magn Reson. 2015;17:59.
88. Heer T, Reiter S, Höfling B, Pilz G. Diagnostic performance of non-contrast-enhanced whole-heart magnetic resonance coronary angiography in combination with adenosine stress perfusion cardiac magnetic resonance imaging. Am Heart J. 2013;166:999–1009.
89. Yoon YE, Kitagawa K, Kato S, et al. Prognostic value of coronary magnetic resonance angiography for prediction of cardiac events in patients with suspected coronary artery disease. J Am Coll Cardiol. 2012;60(22):2316–22.
90. Cheng L, Ma L, Schoenhagen P, Ye H, Lou X, Gao Y, et al. Comparison of three-dimensional volume-targeted thin-slab FIESTA magnetic resonance angiography and 64-multidetector computed tomographic angiography for the identification of proximal coronary stenosis. Int J Cardiol. 2013;167:2969–76.
91. Makowski MR, Henningsson M, Spuentrup E, Kim WY, Maintz D, et al. Characterization of coronary atherosclerosis by magnetic resonance imaging. Circulation. 2013;128:1244–55.
92. Kim WY, Stuber M, Bornert P, Kissinger KV, Manning WJ, Botnar RM. Three-dimensional black-blood cardiac magnetic resonance coronary vessel wall imaging detects positive arterial remodeling in patients with nonsignificant coronary artery disease. Circulation. 2002;106:296–9.
93. Kim WY, Astrup AS, Stuber M, Tarnow L, Falk E, Botnar RM, et al. Subclinical coronary and aortic atherosclerosis detected by magnetic resonance imaging in type 1 diabetes with and without diabetic nephropathy. Circulation. 2007;115:228–35.
94. Jansen CH, Perera D, Makowski MR, Wiethoff AJ, Phinikaridou A, Razavi RM, et al. Detection of intracoronary thrombus by magnetic resonance imaging in patients with acute myocardial infarction. Circulation. 2011;124:416–24.
95. Kawasaki T, Koga S, Koga N, Noguchi T, Tanaka H, Koga H, et al. Characterization of hyperintense plaque with noncontrast T(1)-weighted cardiac magnetic resonance coronary plaque imaging: comparison with multislice computed tomography and intravascular ultrasound. JACC Cardiovasc Imaging. 2009;2:720–8.
96. Noguchi T, Kawasaki T, Tanaka A, Yasuda S, Goto Y, Ishihara M, et al. High-intensity signals in coronary plaques on noncontrast T1-weighted magnetic resonance imaging as a novel determinant of coronary events. J Am Coll Cardiol. 2014;63(10):989–99.
97. Noguchi T, Tanaka A, Kawasaki T, Goto Y, Morita Y, Asaumi Y, et al. Effect of intensive statin therapy on coronary high-intensity plaques detected by noncontrast T1-weighted imaging: The AQUAMARINE Pilot Study. J Am Coll Cardiol. 2015;66:245–56.
98. Yeon SB, Sabir A, Clouse M, Martinezclark PO, Peters DC, Hauser TH, et al. Delayed-enhancement cardiovascular magnetic resonance coronary artery wall imaging: Comparison with multislice computed tomography and quantitative coronary angiography. J Am Coll Cardiol. 2007;50:441–7.
99. Ibrahim T, Makowski MR, Jankauskas A, Maintz D, Karch M, Schachoff S, et al. Serial contrast-enhanced cardiac magnetic resonance imaging demonstrates regression of hyperenhancement within the coronary artery wall in patients after acute myocardial infarction. JACC Cardiovasc Imaging. 2009;2:580–8.
100. Lobbes MB, Miserus RJ, Heeneman S, Passos VL, Mutsaers PH, Debernardi N, et al. Atherosclerosis: contrast-enhanced mr im- aging of vessel wall in rabbit model–comparison of gadofosveset and gadopentetate dimeglumine. Radiology. 2009;250:682–91.
101. Phinikaridou A, Andia ME, Protti A, Indermuehle A, Shah A, Smith A, et al. Noninvasive magnetic resonance imaging evaluation of endothelial permeability in murine atherosclerosis using an albumin-binding contrast agent. Circulation. 2012;126:707–19.
102. Kooi ME, Cappendijk VC, Cleutjens KB, Kessels AG, Kitslaar PJ, Borgers M, et al. Accumulation of ultrasmall superparamagnetic particles of iron oxide in human atherosclerotic plaques can be detected by in vivo magnetic resonance imaging. Circulation. 2003;107:2453–8.
103. Tang TY, Howarth SP, Miller SR, Graves MJ, Patterson AJ, U-King-Im JM, et al. The atheroma (atorvastatin therapy: effects on reduction of macrophage activity) study. Evaluation using ultrasmall superparamagnetic iron oxide-enhanced magnetic resonance imaging in carotid disease. J Am Coll Cardiol. 2009;53:2039–50.
104. Piccini D, Monney P, Sierro C, Coppo S, Bonanno G, van Heeswijk RB, et al. Respiratory self-navigated postcontrast whole-heart coronary MR angiography: initial experience in patients. Radiology. 2014;270:378–86.
105. Stehning C, Börnert P, Nehrke K, Eggers H, Stuber M. Free-breathing whole-heart coronary MRA with 3D radial SSFP and self-navigated image reconstruction. Magn Reson Med. 2005;54:476–80.
106. Piccini D, Bonanno G, Ginami G, Littmann A, Zenge MO, Stuber M. Is there an optimal respiratory reference position for self-navigated whole-heart coronary MR angiography? J Magn Reson Imaging. 2015 July 14. [Epub ahead of print].

107. Ginami G, Bonanno G, Schwitter J, Stuber M, Piccini D. An iterative approach to respiratory self-navigated whole-heart coronary MRA significantly improves image quality in a preliminary patient study. Magn Reson Med. 2015 May 8. [Epub ahead of print].
108. Henningsson M, Koken P, Stehning C, Razavi R, Prieto C, Botnar RM. Whole-heart coronary MR angiography with 2D self-navigated image reconstruction. Magn Reson Med. 2012;67:437–45.
109. Henningsson M, Smink J, Razavi R, Botnar RM. Prospective respiratory motion correction for coronary MR angiography using a 2D image navigator. Magn Reson Med. 2012;69:486–94.
110. Moghari MH, Roujol S, Henningsson M, Kissinger KV, Annese D, Nezafat R, et al. Three-dimensional heart locator for whole-heart coronary magnetic resonance angiography. Magn Reson Med. 2014;71:2118–26.
111. Prieto C, Doneva M, Usman M, Henningsson M, Greil G, et al. Highly efficient respiratory motion compensated free-breathing coronary MRA using golden-step Cartesian acquisition. J Magn Reson Imaging. 2015;41:738–46.
112. Pang J, Bhat H, Sharif B, Fan Z, Thomson LE, LaBounty T, et al. Whole-heart coronary MRA with 100% respiratory gating efficiency: self-navigated three-dimensional retrospective image-based motion correction (TRIM). Magn Reson Med. 2014;71:67–74.
113. Aitken AP, Henningsson M, Botnar RM, Schaeffter T, Prieto C. 100% Efficient three-dimensional coronary MR angiography with two-dimensional beat-to-beat translational and bin-to-bin affine motion correction. Magn Reson Med. 2015;74:756–64.
114. Lustig M, Donoho DL, Pauly JM. Sparse MRI: the application of compressed sensing for rapid MR imaging. Magn Reson Med. 2007;58(6):1182–95.
115. Henningsson M, Prieto C, Chiribiri A, Vaillant G, Razavi R, Botnar RM. Whole-heart coronary MRA with 3D affine motion correction using 3D image-based navigation. Magn Reson Med. 2014;71:173–81.
116. Akçakaya M, Rayatzadeh H, Basha TA, et al. Accelerated late gadolinium enhancement cardiac MR imaging with isotropic spatial resolution using compressed sensing: initial experience. Radiology. 2012;264:691–9.
117. Akcakaya M, Basha TA, Goddu B, Goepfert LA, Kissinger KV, Tarokh V, et al. Low-dimensional-structure self-learning and thresholding: regularization beyond compressed sensing for MRI Reconstruction. Magn Reson Med. 2011;66:756–67.
118. Akcakaya M, Basha TA, Chan RH, Rayatzadeh H, Kissinger KV, Goddu B, et al. Accelerated contrast-enhanced whole-heart coronary MRI using low-dimensional-structure self-learning and thresholding. Magn Reson Med. 2012;67:1434–43.
119. Akçakaya M, Basha TA, Chan RH, et al. Accelerated isotropic sub-millimeter whole-heart coronary MRI: compressed sensing versus parallel imaging. Magn Reson Med. 2014;71:815–22.
120. Moghari MH, Akçakaya M, O'Connor A, Basha TA, Casanova M, Stanton D, et al. Compressed-sensing motion compensation (CosMo): a joint prospective-retrospective respiratory navigator for coronary MRI. Magn Reson Med. 2011;66:1674–81.
121. Forman C, Piccini D, Grimm R, Hutter J, Hornegger J, Zenge MO. Reduction of respiratory motion artifacts for free-breathing whole-heart coronary MRA by weighted iterative reconstruction. Magn Reson Med. 2015;73(5):1885–95.
122. Coppo S, Piccini D, Bonanno G, Chaptinel J, Vincenti G, Feliciano H, et al. Free-running 4D whole-heart self-navigated golden angle MRI: initial results. Magn Reson Med. 2014 Nov 5. [Epub ahead of print].
123. Pang J, Sharif B, Fan Z, Bi X, Arsanjani R, et al. ECG and navigator-free four-dimensional whole-heart coronary MRA for simultaneous visualization of cardiac anatomy and function. Magn Reson Med. 2014;72:1208–17.